



Ministry of Higher Education and Scientific Research
Kasdi Merbah Ouargla University
Faculty of New Information and Communication Technologies
Department of Electronics and Telecommunications

Dissertation

ACADEMIC MASTER

Domain: Sciences and Technologies

Track: Telecommunications

Specialty “Telecommunication systems”

**Design and study of a 2D photonic crystal biosensor for
detection of blood components**

Presented and publicly defended by

Terea Hadda Nour El Houda and Boudi Noura

On 24-06-2024

Jury

Hamza OTHMANI,

Mohammed BOULESBAA,

Boualem MEKIMAH,

Rima HADJADJ,

MCA at the University of Ouargla

Professor at the University of Ouargla

MCA at the University of Ouargla

A doctoral student at the University of Ouargla

President

Supervisor

Examiner

Guest

Dedication

Thank God for the joy of fulfillment and thank God at the beginning and at the end.

To **my father**, who illuminated my paths and my model with every step I took.

To **my affectionate mother**, warm hugs and my heaven that has never left me, and my day is not complete without her.

To **my brothers** and **sisters** who have always supported me and supported me throughout my educational career.

To all my dear teachers who have taught and guided me.

I dedicate this humble work and the fruit of my efforts to all of you, and God bless me.

Noura

Dedication

I thank my Almighty God for giving me the strength and courage to complete his studies.

To your dearest parents who are always sacrificed to see me succeed, may God grant them good health and long life.

To all my brothers, **Sadek, Bachir, Nouraldin.**

To all my sisters, **Nedjma, safaa, malaak.**

To my nephews, **Ritaj, Wadih .**

And I dedicate this work to my friends, all my relatives.

I dedicate this work to everyone who helped me from near and far.

Hadda Nour Elhouda

Acknowledgements

We thank Allah the Almighty for giving us the courage, the will, the health, and the patience, so that, during all these years of study, we can get to where we are today and exploit all our efforts for this modest work.

We want to thank our supervisor, **Pr. Mohammed BOULESBAA**, professor at the University of Ouargla, for his kindness, his trust, his advice and his constant support to carry out this letter.

We thank the members of the jury **Dr. Boualem Mekimah** senior lecturer of Class A and **Dr. Hamza Othmani** class A lecturer for agreeing to evaluate this graduation work.

We would like to express to **Mrs. Rima Hadjadj**, PhD student at the University of Ouargla, all our gratitude for the honor she has done for us.

Our thanks are also addressed to our Department of Electronics and Telecommunications teachers for their contributions to our training.

We especially thank **Dr. Tamer Saleh El-Sayed Mostafa**, Assistant Professor Telecommunication in Department -Egyptian Russian University(ERU) for the help and advice he gave us throughout this work.

Finally, we thank our families, our friends and all those who, from near or far, have contributed to the realization of this work.

Résumé

Dans ce mémoire, nous avons proposé et conçu, et analysé une structure d'un biocapteur à base de cristaux photoniques PhC-2D de biomolécules à base d'une cavité couplée à un guide d'ondes. Ce travail a été réalisé avec des distributions circulaires de tiges de silicium d'indice de réfraction de 3,46 RIU, dans un fond d'air d'indice de réfraction de 1 RIU, puis en calculant la bande interdite par la méthode PWE, et en analysant les résultats à l'aide de FDTD, nous avons travaillé sur l'application de la détection des composants sanguins, et nous nous sommes appuyés pour améliorer la détection de la structure en changeant le nombre de tiges de mesure. Les résultats ont montré qu'avec une augmentation du nombre de tiges de mesure, la sensibilité augmentait, car nous avons obtenu le facteur de qualité le plus élevé de 1236,83 et un facteur de mérite allant jusqu'à 65,14 $(\text{RIU})^{-1}$ à N=18 tige et une sensibilité maximale de 124,83 nm/RIU à N=54 tige.

Mot clé : biocapteur; cristaux photoniques;Tiges de mesure; Le facteur de qualité; Sensibilité; PWE; FDTD.

Abstract

In this dissertation, we proposed and simulated hexagonal structures of a biosensor based on photonic crystals PC-2D of biomolecules based on a cavity coupled with a waveguide. This work was carried out with circular distributions of silicon rods with a refractive index of 3.46 RIU, in a background of air with a refractive index of 1 RIU, then calculated the band gap by the PWE method, and analyzing the results using FDTD, we worked on the application of detection of blood components and relied in improving the structure on changing the number of measuring rods. The results showed that with an increase in the number of measuring rods, the sensitivity increased, as we obtained the highest quality factor of 1236.83 and a merit factor of up to 65.14 $(\text{RIU})^{-1}$ at N=18 rods and a maximum sensitivity of 124.83 nm/RIU at N=54 rods.

Keywords : biosensor; photonic crystals; Measuring rods; The quality factor;Sensitivity; PWE; FDTD.

ملخص

في هذه الاطروحة، قمنا باقتراح ومحاكاة بني سداسية لجهاز استشعار حيوي على أساس البلورات الفوتونية 2D-PhC للجزئيات الحيوية يستند على تجويف مقترن بدليل موجي . تم تنفيذ هذا العمل بتوزيعات دائرية لقضبان من السيلكون مع معامل انكسار RIU 3.46 ، في خلفية من الهواء مع معامل انكسار RIU 1 ، ثم حساب فجوة النطاق بطريقة (PWE) وتحليل النتائج باستخدام (FDTD) ، لقد عملنا على تطبيق كشف مكونات الدم ، واعتمدنا في تحسين الهيكل على تغيير عدد اقضاب القياس . أظهرت النتائج أنه عند الزيادة في عدد اقضاب القياس زادت الحساسية حيث تحصلنا على اعلى عامل جودة 1236.83 وعامل جدارة يصل 65.14 RIU^{-1} عند $N = 18$ قضيب والحساسية قصوى 124.94 نانومتر / RIU عند $N = 54$ قضيب.

كلمات مفتاحية : جهاز استشعار حيوي ؛ البلورات الفوتونية؛ قضبان القياس؛ عامل الجودة؛ الحساسية؛ PWE ؛ FDTD .

Contents

| | |
|--|-------------|
| Dedication | ii |
| Dedication | iii |
| Acknowledgements | iv |
| Contents | vii |
| List of figures | x |
| List of Tables | xii |
| List of acronyms | xiii |
| List of symbols | xiv |
| General introduction | 1 |
| 1 Photonic Crystals: Introduction & presentation | 4 |
| 1.1 Introduction | 5 |
| 1.2 Definition | 5 |
| 1.3 Type of photonic crystals | 6 |
| 1.3.1 Natural photonic crystals | 6 |
| 1.3.2 Artificial photonic crystals | 6 |
| 1.3.2.1 One-dimensional photonic crystals CPs-1D | 7 |
| 1.3.2.2 Two-dimensional photonic crystals (CPs -2D) | 7 |
| 1.3.2.3 Three-dimensional photonic crystals (CPs-3D) | 8 |
| 1.4 Main characteristics of photonic crystals | 9 |
| 1.4.1 The index contrast | 9 |
| 1.4.2 The period | 9 |
| 1.4.3 The filling factor | 9 |
| 1.5 Polarization of the electromagnetic wave (TE and TM) | 10 |
| 1.5.1 Diagrams of bands | 10 |
| 1.6 Different type of defects in photonic crystals | 11 |
| 1.6.1 One-off defects | 11 |
| 1.6.2 Linear defects | 11 |
| 1.7 Cavities with photonic crystals | 12 |
| 1.7.1 Point cavities | 12 |
| 1.7.2 Hetero -structural cavities | 12 |
| 1.8 Cavity structures with local modulation of linear defect width | 13 |
| 1.9 Photonic crystal waveguide | 14 |

| | | |
|----------|--|-----------|
| 1.10 | Guide/cavity coupling in a 2D photonic crystal | 15 |
| 1.11 | Applications of photonic crystals | 15 |
| 1.12 | Conclusion | 16 |
| 2 | Introduction to sensors based on photonic crystals | 17 |
| 2.1 | Introduction | 18 |
| 2.2 | Definition | 18 |
| 2.3 | Classification of sensors | 19 |
| 2.3.1 | Active sensors | 19 |
| 2.3.2 | Passive sensors | 19 |
| 2.4 | Photonic crystal sensors | 20 |
| 2.5 | Various types of sensors | 20 |
| 2.5.1 | Physical sensor | 20 |
| 2.5.2 | Chemical sensor | 21 |
| 2.5.3 | Optical sensor | 21 |
| 2.6 | Biosensor | 21 |
| 2.6.1 | Operating Principle | 21 |
| 2.7 | Different Types of Biosensors | 22 |
| 2.8 | Basic characteristics of the biosensor | 22 |
| 2.8.1 | Selectivity | 22 |
| 2.8.2 | Reproducibility | 23 |
| 2.8.3 | Stability | 23 |
| 2.8.4 | sensitivity | 23 |
| 2.8.5 | Linearity | 23 |
| 2.9 | Optical biosensor | 24 |
| 2.9.1 | Optical biosensors with photonic crystals | 24 |
| 2.10 | Applications of Biosensors | 25 |
| 2.11 | Conclusion | 25 |
| 3 | Design of a PC-2D based biosensor for the detection of blood components | 26 |
| 3.1 | Introduction | 27 |
| 3.2 | Performance parameters | 27 |
| 3.3 | The mechanism of action of PCs sensor for the detection of biomolecules | 28 |
| 3.4 | PC-2D hexagonal lattice structure | 28 |
| 3.5 | Photonic bandgap analysis | 29 |
| 3.6 | Design of a PC biosensor based on a cavity coupled to a waveguide | 29 |
| 3.7 | Distribution of the electric field | 30 |
| 3.8 | Transmission spectrum of the biosensor | 31 |
| 3.9 | How biomolecules attach to measuring rods | 31 |
| 3.10 | Simulation results | 32 |
| 3.11 | Conclusion | 37 |
| 4 | Optimization of the sensitivity of the PC biosensor by varying the number of measuring rods | 38 |
| 4.1 | Introduction | 39 |
| 4.2 | Optimization of the biosensor based on photonic crystals by the number of measuring rods | 39 |
| 4.2.1 | Case1: Number of rods connected to the biomolecules is 9 rods | 39 |
| 4.2.2 | Case2: Number of rods connected to the biomolecules is 12 rods | 40 |

| | | |
|-------|--|-----------|
| 4.2.3 | Case3: Number of rods connected to the biomolecules is 18 rods . . . | 42 |
| 4.2.4 | Case4: Number of rods connected to the biomolecules is 54 rods . . . | 43 |
| 4.3 | Comparison of the proposed biosensor with different designs with PCs bases | 47 |
| 4.4 | Conclusion | 47 |
| | General conclusion | 48 |

List of figures

- 1.1 Various photonic crystal structures of different dimensions. 5
- 1.2 Examples of Natural photonic crystals 6
- 1.3 Examples of artificial photonic crystals 6
- 1.4 One-dimensional (1D) photonic crystal or belayedsuper lattice with period-
icity in Z direction. 7
- 1.5 Connected 2D periodic structure. 8
- 1.6 Disconnected 2D periodic structure. 8
- 1.7 (a) SEM image of a Woodpile structure; (b) The Yablonovite, named after its
designer, one of the first 3D structures. 8
- 1.8 Periods of a one-dimensional photonic crystal. 9
- 1.9 Transverse magnetic TM and transverse electric TE polarization. 10
- 1.10 Band structure diagram for a two-dimensional crystal 11
- 1.11 Examples of simple one-time defects. (a) Deficiency. (b) Atom in interstitial
position.(c) Atom in the substitutional position. 11
- 1.12 Diagram of a fault guide in a lattice (a) of rods of a dielectric (b) of air holes. 12
- 1.13 Scanning electron microscope (SEM) image of an L3-type cavity manufact-
ured at the IEF 13
- 1.14 (a) Double hetero-structure cavity, made by connecting the basic structures
with photonic crystals, I and II. The photonic crystal I has a triangular lattice
structure with a lattice constant a_1 . The photonic crystal II has a triangular
grating structure deformed into a rectangular grating with centered faces
with a constant $a_2 (>a_1)$ in the direction of the waveguide. It has the same
constant as that of the photonic crystal I in the orthogonal direction in order
to satisfy the adaptation conditions of mesh. 13
- 1.15 Diagram of an example of a cavity with linear defect width modulation. The
displacement of the holes has been exaggeratedly increased for a better un-
derstanding. 14
- 1.16 Examples of linear defects in a photonic crystal² created (a) by omitting a
single row of patterns, (b) by modifying the refractive index of a single row
of patterns, (c) by varying the radius of a single row of patterns of the structure. 14
- 1.17 Passive and active devices associating guide and cavity of the same photonic
crystal. 15

- 2.1 Principle of a sensor. 18
- 2.2 Constitution of a sensor. 19
- 2.3 General principle of a biosensor 21
- 2.4 Schematic diagram of biosensor comprising three components: detector,
transducer and output system. 22

| | | |
|------|--|----|
| 2.5 | A diagram showing the different types of biosensors classified. | 22 |
| 2.6 | Schematic structure of optical detection system. | 24 |
| 2.7 | Applications of Biosensors. | 25 |
| 3.1 | The diagram of the hexagonal structure used for the biosensor design is based on 2D-PCs. | 28 |
| 3.2 | Presents a diagram of photonic bandgaps of the hexagonal grating structure in PC. | 29 |
| 3.3 | Biosensor structure designed with a cavity. | 30 |
| 3.4 | Distribution of the electric field in 2D of biosensor based with on a resonant cavity (b) frequency-denoted biosensor transmission spectrum (c) the transmission spectrum of biosensor in terms of the resonance wavelength. | 30 |
| 3.5 | (a) frequency-denoted biosensor transmission spectrum (b) the transmission spectrum of biosensor in terms of the resonance wavelength. | 31 |
| 3.6 | Biosensor structure designed with a cavity and biomolecules | 32 |
| 3.7 | Biosensor output in reference mode (air). | 32 |
| 3.8 | Biosensor output for Water. | 33 |
| 3.9 | Biosensor output for Blood Plasma. | 33 |
| 3.10 | Biosensor output for Ethanol. | 34 |
| 3.11 | Biosensor output for Sylgard184-Glucose. | 34 |
| 3.12 | Biosensor output for Polyacrylamide. | 35 |
| 3.13 | Biosensor output for Bovine-Serum-Albumin. | 35 |
| 3.14 | Biosensor output for Urethame-Dimethacrylate. | 36 |
| 3.15 | The resonance wavelength spectra produced at various blood components with refractive indices. | 36 |
| 4.1 | The structure of the biosensor for 9 measuring rods. | 39 |
| 4.2 | The transmission spectra of the biosensor for 9 functional rods. | 40 |
| 4.3 | The structure of the biosensor for 12 measuring rods. | 41 |
| 4.4 | The transmission spectra of the biosensor for 12 functional rods. | 41 |
| 4.5 | The structure of the biosensor for 18 measuring rods. | 42 |
| 4.6 | The transmission spectra of the biosensor for 18 functional rods. | 43 |
| 4.7 | The structure of the biosensor for 54 measuring rods. | 44 |
| 4.8 | The transmission spectra of the biosensor for 54 functional rods. | 44 |
| 4.9 | The evolution of the quality factor and sensitivity about the number of functional rods (N). | 45 |
| 4.10 | Sensitivity to the biosensor as a function of the number of measuring rods (N) for the optimal structure of the biosensor. | 46 |
| 4.11 | (a) Sensitivity mass curve regarding the number of measuring rods. (b) curve the relationship between the wavelength of the variable resonance and the number of measuring rods. | 47 |

List of Tables

| | | |
|-----|---|----|
| 2.1 | The effect used on the measurand to realize the output magnitude. [38]. . . | 19 |
| 2.2 | Output Quantity Results by Selected Measures and Materials Used [39]. . . . | 20 |
| 3.1 | Optical and geometric parameters of the hexagonal structure based on PCs. | 29 |
| 3.2 | Sensor output according to biomolecules connected to the measuring rods. | 37 |
| 4.1 | Summarizes the results obtained by the biosensor during the conduction of refractive indices of blood components in the case of N=9. | 40 |
| 4.2 | Summarizes the results obtained by the biosensor during the conduction of refractive indices of blood components in the case of N=12. | 42 |
| 4.3 | Summarizes the results obtained by the biosensor during the conduction of refractive indices of blood components in the case of N=18. | 43 |
| 4.4 | Summarizes the results obtained by the biosensor during the conduction of refractive indices of blood components in the case of N=54. | 45 |
| 4.5 | comparison of the results of the main parameters of the studied structures at Urethane-Dimethacrylate. | 46 |
| 4.6 | Results of previous studies compared to the results obtained. | 47 |

List of acronyms

| | |
|-------|--|
| PBG | photonic band gap. |
| PC | Photonic crystal. |
| PCs | Photonic crystals. |
| 1D | one-dimensional . |
| 2D | two-dimensional . |
| 3D | three-dimensional . |
| f | The filling factor . |
| L_n | linear cavities. |
| H_n | hexagonal cavities. |
| SEM | scanning electron microscope. |
| Q | The quality factor. |
| DNA | deoxyribonucleic acid. |
| PWE | Plane Wave Expansion. |
| FDTD | Finite-Difference Time-Domain. |
| S | sensitivity. |
| DL | detection limit . |
| FOM | merit factor. |
| TE | Transverse Electric, TE polarization . |
| TM | Transverse Magnetic, TM polarization. |
| si | Silicon. |
| LEDs | Light-emitting diodes. |
| LASER | Light Amplification by Stimulated Emission of Radiation. |
| RIU | Refractive Index Unit. |

List of symbols

| | |
|----------------|---|
| Δ_n | Refractive index differences . |
| $\epsilon(z)$ | Dielectric function . |
| z | According to adirection . |
| λ | Wavelength. |
| λ_0 | Resonance wavelength. |
| ΓK | The direction of the reciprocal network corresponds to the direction of the first neighbors of the real network . |
| a | Period of the photonic crystal. |
| r | Radius of the photonic crystal. |
| V | volume. |
| R | Reflectivity. |
| n | Refractive index. |
| ϵ | Dielectric permittivity. |
| ω | The pulsation. |
| V | The potential. |
| y | The output signal. |
| c | The analyte concentration. |
| m | The sensitivity of the biosensor. |
| Λ | Cell volume. |
| Δ | The index contrast. |
| E | the electric field. |
| H | the magnetic field. |
| $\Delta\omega$ | The pulsation differences . |

General introduction

New technologies have been developed due to advancements in photonics and nanotechnology, and these developments have revolutionized several industries, including biological diagnosis and detection. The field of photonics, which involves using light to transmit and manipulate information, has seen significant breakthroughs that enable more precise and efficient diagnostic tools. Nanotechnology, which deals with the manipulation of matter on an atomic or molecular scale, has also contributed to the creation of innovative materials and devices. Together, these disciplines have led to the development of photonic crystals, which are materials that can control the flow of light. These photonic crystals have numerous applications in medical diagnostics, allowing for more accurate detection of diseases at earlier stages. Furthermore, advancements in photonic and nanotechnology have improved imaging techniques, making it possible to observe biological processes in greater detail than ever before. This synergy between photonics and nanotechnology continues to drive progress in various fields, promising even more revolutionary changes in the future.

Photonic crystals [1, 2] are characterized by a periodic variation of the refractive index in one, two, or three dimensions. They primarily exhibit properties related to the presence of forbidden bands that prevent the propagation of waves in any direction of the incident wave [3, 4]. These prohibited bands are utilized to design position modes that confine light energy. Introducing a defect, whether exact, linear, or both, into these structures makes it possible to disrupt the periodicity and, consequently, the continuity of the wave propagation, allowing for the precise control of light within the defect zone. This capability can be harnessed in various applications, including integrated optics [5], splitters [6–8], lasers [9], LEDs [10], sensors [11, 12], and biosensors [13, 14]. PC sensors are artificial devices with exceptional optical characteristics, representing a promising technology in medicine. These sensors leverage the properties of light to perform various functions, making them highly effective for precise and efficient detection. PC sensors can detect these molecules accurately and efficiently when combined with biomolecules. A biosensor [15] is a photonic device that identifies and measures chemical substances and molecules. These biosensors are crucial in various applications, including medical diagnostics, environmental monitoring, and food safety, because they provide rapid and reliable results [16]. PC biosensors operate by guiding light and detecting variations in the refractive index of biomolecules. These changes can be measured through various signals, including the intensity of the light, the wavelength spectrum, and its polarization. Such detailed analysis allows for precise detection and monitoring of biological substances. Among the numerous applications of PC biosensors in the field of medicine are cancer detection, where they can identify malignant cells at an early stage [17], DNA analysis, which benefits from their high sensitivity and specificity [18], and the detection of blood components [19], providing crucial information for diagnostics and treatment monitoring. Additionally, photonic biosensors have been employed in identifying viral infections, such as the chikungunya virus, demonstrating their versatility and potential in managing public health challenges [20].

This dissertation aims to develop and design a biosensor structure based on two-dimensional photonic crystals to detect blood components. In our work, we have designed a biosensor based on 2D photonic crystals. This PC biosensor is based on the coupling of a waveguide with a resonant cavity. For this biosensor, we used a hexagonal 2D lattice composed of 15 x 15 circular silicon rods integrated in an air bottom along the X and Z axes, respectively. To achieve good performance in terms of PWE, FDTD.

In the first chapter, we will give an overview of photonic crystals. Next, we will describe

the different forms of photonic crystals, their types, and their characteristics. It will also bypass the defects and cavities that can occur in photonic crystals. Finally, we will conclude this chapter with an exposition of certain applications of photonic crystals.

In the second chapter we will give a complete overview of sensors and biosensors, focusing on the main characteristics and uses that help us understand how these devices work. We will pay particular attention to biosensors that use photonic crystals.

In the third chapter, we will design a structure of a biosensor based on photonic crystals. Our study aims to improve the detection of biomolecules by exploiting the differences in their refractive indices in the application of the detection of blood components and we will perform in depth calculations to divide the different key parameters as a quality factor, sensitivity, DL and FOM.

In the last chapter of this note, we will study the structure of the previous biosensor by means of a change in the measuring rods with a view to its development. Using the same previous application we will present in detail the results of our simulations, and we will finish the chapter in comparison with the results of previous research.

Finally, we will conclude our work with a general conclusion and prospects for future work.

Chapter 1

Photonic Crystals: Introduction & presentation

Contents

| | |
|---|-----------|
| 1.1 Introduction | 5 |
| 1.2 Definition | 5 |
| 1.3 Type of photonic crystals | 6 |
| 1.3.1 Natural photonic crystals | 6 |
| 1.3.2 Artificial photonic crystals | 6 |
| 1.4 Main characteristics of photonic crystals | 9 |
| 1.4.1 The index contrast | 9 |
| 1.4.2 The period | 9 |
| 1.4.3 The filling factor | 9 |
| 1.5 Polarization of the electromagnetic wave (TE and TM) | 10 |
| 1.5.1 Diagrams of bands | 10 |
| 1.6 Different type of defects in photonic crystals | 11 |
| 1.6.1 One-off defects | 11 |
| 1.6.2 Linear defects | 11 |
| 1.7 Cavities with photonic crystals | 12 |
| 1.7.1 Point cavities | 12 |
| 1.7.2 Hetero -structural cavities | 12 |
| 1.8 Cavity structures with local modulation of linear defect width | 13 |
| 1.9 Photonic crystal waveguide | 14 |
| 1.10 Guide/cavity coupling in a 2D photonic crystal | 15 |
| 1.11 Applications of photonic crystals | 15 |
| 1.12 Conclusion | 16 |

1.1 Introduction

Technological progress based on light and the study of light has become an economic and social need in the 21st century. Photonics has influenced various scientific and technological fields, including medical diagnostics and communications. The idea of "photonic crystals" was first born in 1987 by John and pabloventich [21] [22], it was made in 1991. Optical crystals are considered to be structures whose refractive index varies periodically on the wavelength scale in one or more directions. They are divided into two categories: natural and artificial optical crystals. In this chapter, we first present the general information about natural and artificial optical crystals. Next, the optical properties of photonic crystals. And we reveal the different types of their defects and the different structures based on photonic crystals will also be discussed. Finally, different applications will be presented about them.

1.2 Definition

Photonic crystals (PCs) are periodic microscopic structures that affect the flow of photons in the same way as an ionic lattice affects electrons in semiconductors. PCs are periodic dielectric structures [23]. They are named as crystals because of their frequency and photonic because they act on light. A photonic crystal may block the flow of a certain range of wavelengths in one direction or in all directions, there by providing the possibility of directing, confining and locking light in a cage [21]. A photonic crystal includes repeating regions with a higher and lower dielectric constant that are periodic, Photons propagate through this structure. Modes are the wavelengths allowed to propagate and a set of patterns forming bands [24]. Non-allowable wavelength ranges from photonic band gaps. It prohibits light of some wavelength within the photonic band gap from propagating in any direction within a photonic crystal. They can be created from almost any material, so they meet the requirements for material compatibility [25]. A photonic crystal can be manufactured as a one-dimensional (1D), two-dimensional (2D) and three-dimensional (3D). Figure 1.1 shows the various photonic crystal structures of different dimensions. In (1D) photonic crystal, the periodicity of the refractive index (n) adjustment occurs only in one axis, while the refractive index differences (Δn) are uniform for the other two directions of the structure. Similarly in a two- and three-dimensional photonic crystal, periodic adjustment of the refractive index occurs in two and three axes, respectively.

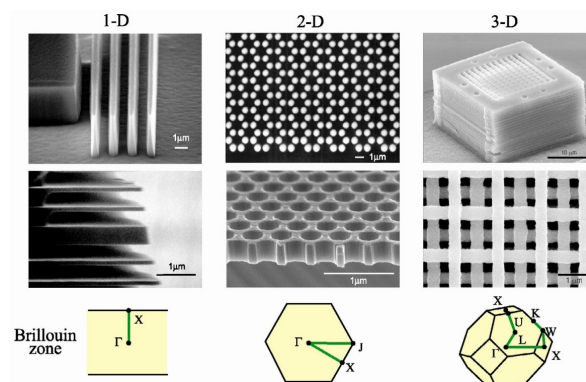


Figure 1.1: Various photonic crystal structures of different dimensions.

1.3 Type of photonic crystals

1.3.1 Natural photonic crystals

Natural photonic crystals are fantastic structures found in nature that control the behavior of light through their complex and periodic microstructures or nanostructures. Unlike conventional crystals formed by atoms, these patterns result from arrangements of materials with different refractive indices. figure 1.2 provides Examples of natural photonic crystals such as Butterfly wings ,Peacock,feathers,Beetles,Opals.

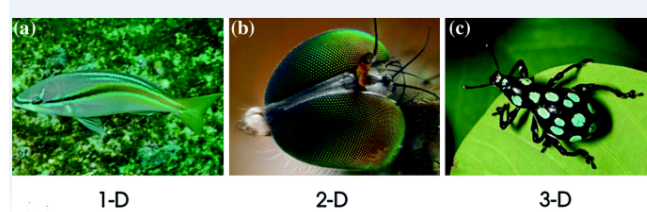


Figure 1.2: Examples of Natural photonic crystals

1.3.2 Artificial photonic crystals

According to the type of structure, three classes of artificial photonic crystals are distinguished the figure 1.3:

- One-way periodicity: 1 D photonic crystal.
- Two-way periodicity of space: 2D photonic crystal .
- Periodicity in all directions of Space: 3D photonic crystal.

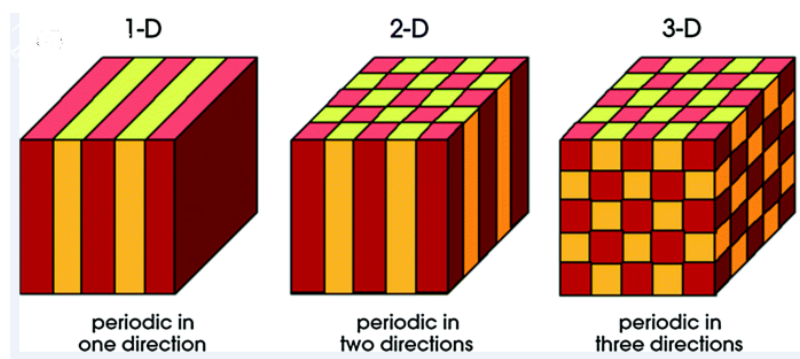


Figure 1.3: Examples of artificial photonic crystals

1.3.2.1 One-dimensional photonic crystals CPs-1D

The simplest structure of photonic crystals is a periodic structure one-dimensional also called "mirrors of Bragg" see figure 1.4, composed of two layers (A, B) or several layers. The reason why it is compared to a one-dimensional photonic crystal is that the unique characteristics of photonic crystals exist only in one dimension. the term one-dimensional is used because the dielectric function $\epsilon(z)$ changes only according to a direction (z) and the other two directions are uniform [26].

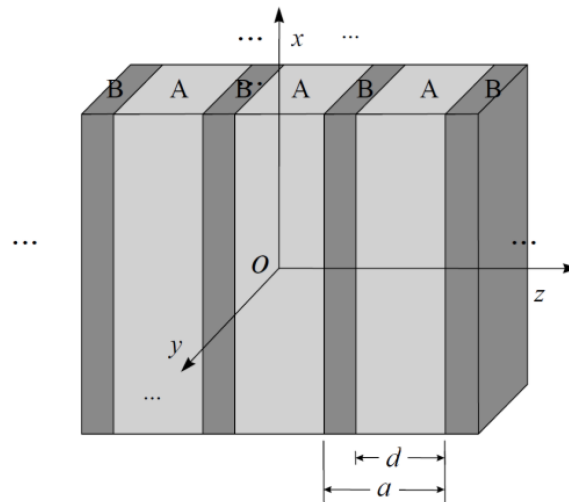


Figure 1.4: One-dimensional (1D) photonic crystal or Bragg super lattice with periodicity in Z direction.

1.3.2.2 Two-dimensional photonic crystals (CPs -2D)

A two-dimensional photonic crystal is structures that has a periodic adjustment of the dielectric permittivity in two directions of space, and is homogeneous with the third. These crystals are highly dependent on the polarization of the electromagnetic wave. Some ways to make these two-dimensional structures:

- **The connected structure**

The elementary patterns have an index n_1 lower than the index n_2 . These structures are usually consisting of a periodic network of air holes drilled in a Silicon matrix see figure 1.5

- **The disconnected structure**

In this structure, the elementary patterns are of index n_1 greater than the index n_2 , it is consisting of dielectric or metal rods aligned periodically in the air or the foam. see figure 1.6

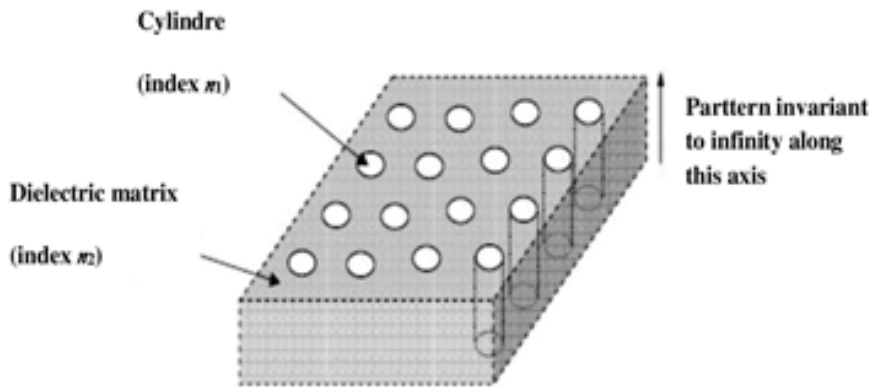


Figure 1.5: Connected 2D periodic structure.

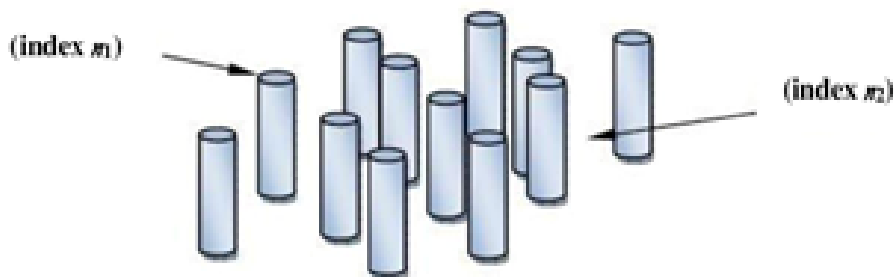


Figure 1.6: Disconnected 2D periodic structure.

1.3.2.3 Three-dimensional photonic crystals (CPs-3D)

Structures whose dielectric permittivity is periodically structured in the three directions. That is, at each frequency, propagation is possible in all directions. Its objective is to obtain a complete band gap for all directions of space in order to prevent the spontaneous emission of light. figure 1.7

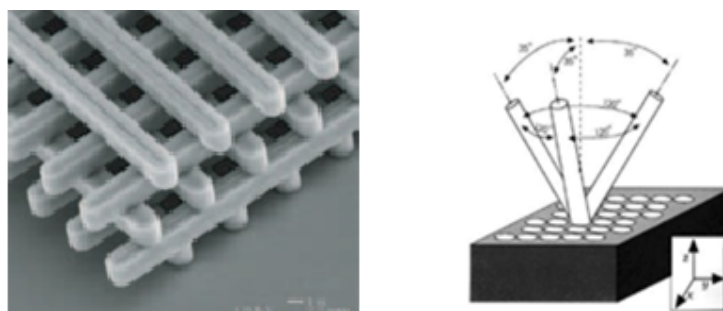


Figure 1.7: (a) SEM image of a Woodpile structure; (b) The Yablonovite, named after its designer, one of the first 3D structures.

1.4 Main characteristics of photonic crystals

A photonic crystal is characterized by the different materials that compose it, the systemcrystalline according to which these materials are organized and the relative volumes they occupy in the elementary cell of the crystal.

1.4.1 The index contrast

The index contrast Δ_n is the difference between the refractive indices of the two materials [27]. It is given by equation 1.1:

$$\Delta_n = n_h - n_l \quad (1.1)$$

with :

n_h : The refractive index of the high index material.

n_l : The refractive index of the low index material.

1.4.2 The period

The choice of the period depends on the frequency domain studied see figure 1.8. This parameter influences the width or the aperture of the photonic band gap. The period (a) is given by 1.2:

$$a = (a_1 + a_2) \quad (1.2)$$

with :

a_1 : the thickness of the layer of index n_1 .

a_2 : the thickness of the layer of index n_2 .

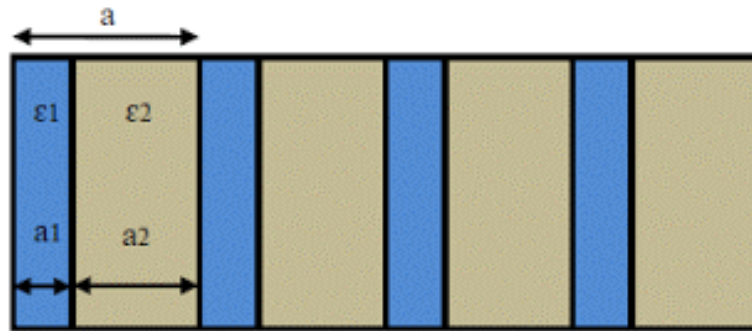


Figure 1.8: Periods of a one-dimensional photonic crystal.

1.4.3 The filling factor

The filling factor (f) is defined as being the ratio between the volume occupied by this material in the elementary cell of the crystal and the volume of the elementary cell. For a planar two-dimensional photonic crystal composed of air holes drilled in a dielectric matrix, the air filling factor f designates the ratio between the area of the pattern and the area of the elementary cell of the network considered [28] 1.3

$$f = \frac{A_{pattern}}{A_{elementary pattern}} \quad (1.3)$$

1.5 Polarization of the electromagnetic wave (TE and TM)

The polarization of the light affects the CPs-2D dispersion equations. The electromagnetic field in this instance has been described by two separate polarizations, the Transverse Electric (TE) polarization and the Transverse Magnetic (TM) polarization see figure 1.9. The H field in TE polarization has a single component normal to the plane, and the E field is orientated in the periodicity plane. The electromagnetic field has three components: E_x , E_y , and H_z , with zero for the other components. The field in TM polarization has the form (H_x, H_y, E_z) , with the functions of E and H reversed. With (r) representing the hole radius and (a) representing the lattice period, we consider a triangular lattice of air holes in a dielectric matrix with $\epsilon = 12$. Therefore, electromagnetic waves in 2D crystals can be classified into two polarizations, TE and TM, and propagate in the plane perpendicular to the rods. To create a total band gap, the band gaps that arise in each scenario must overlap [27].

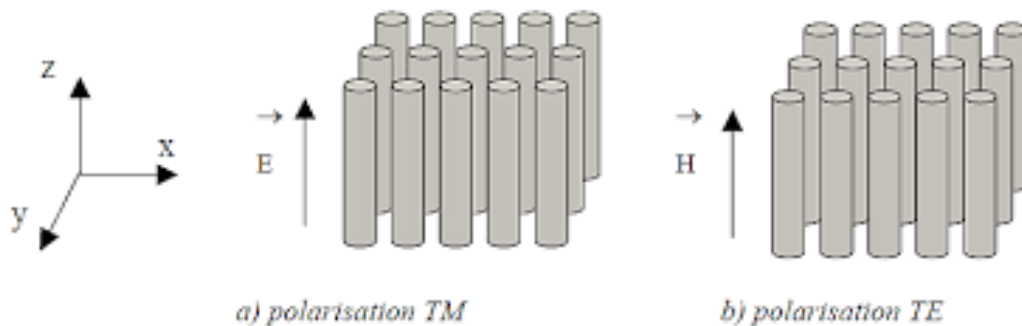


Figure 1.9: Transverse magnetic TM and transverse electric TE polarization.

1.5.1 Diagrams of bands

The photonic band gap (PBG), which is comparable to band gaps or energy gaps for electrons traveling in semiconductors, is one of the most significant characteristics of photonic crystals. The wave-like properties of electrons cause a band gap in semiconductors. Every atom in a semiconductor experiences a periodic potential that electrons as waves encounter and are reflected by. Electrons with specific wave vectors and energies can form standing waves under particular circumstances. The "band gap" is the region of energy where electrons are not permitted to exist. This behavior sets semiconductors apart from insulators and metals. Similarly, electromagnetic standing waves can pass through a periodic structure whose minimal characteristics are smaller than the light's wavelength. Here, photons with specific wavelengths and wave vectors are expelled by the medium. This type of structure is known as a "photonic band gap" because it works as an insulator of light. [29].

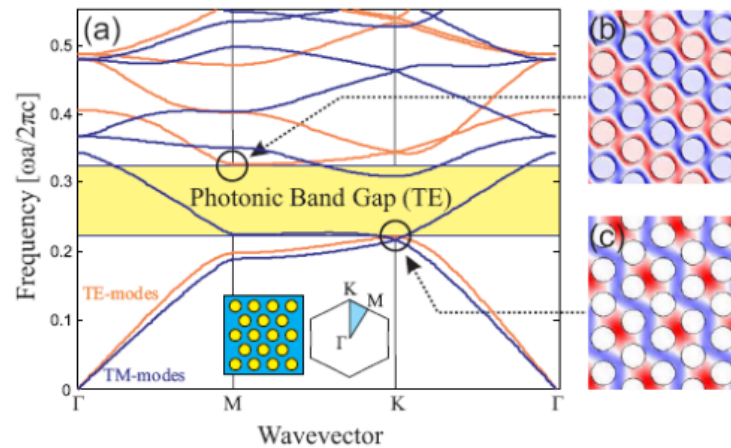


Figure 1.10: Band structure diagram for a two-dimensional crystal

1.6 Different type of defects in photonic crystals

Several types of defects are possible and make it possible to carry out certain applications, such as high selectivity filters, since only the electromagnetic wave whose frequency corresponds to that of the authorized mode will be transmitted or even tunable filters. The imperfection in the periodic arrangement of the dielectric structure is a simple way to create one or more modes allowed in the gap is to introduce a defect in the crystal. In the case of two-dimensional photonic crystals, which are of particular interest to us in this work, several types of defects can be considered.

1.6.1 One-off defects

Point defects in photonic crystals are created either by removing, adding, or modifying one or more crystals [1.11](#)

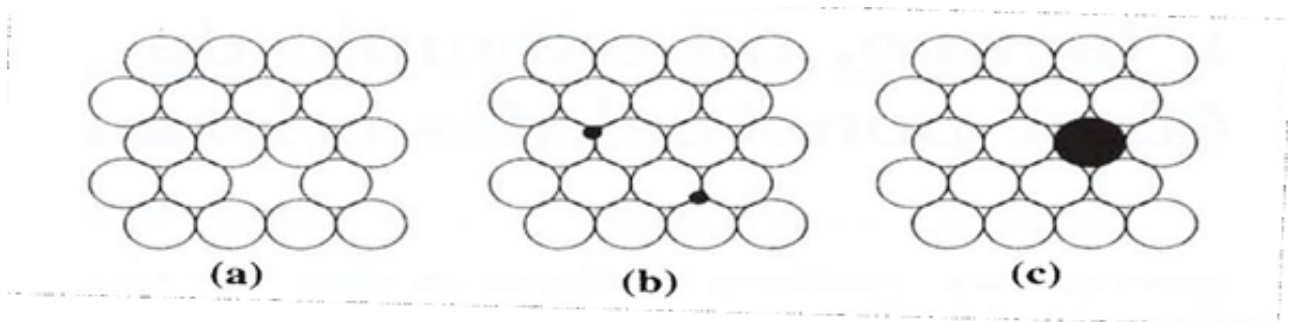


Figure 1.11: Examples of simple one-time defects. (a) Deficiency. (b) Atom in interstitial position. (c) Atom in the substitutional position.

1.6.2 Linear defects

A proof is a linear defect that is introduced inside a light crystal if we reduce to a two-way periodicity in space. A 2D photonic crystal consists of insulating columns sur-

rounded by air, or air holes drilled through an insulating Matrix. A waveguide can then be created by separating the two half-levels in Figure 1.12

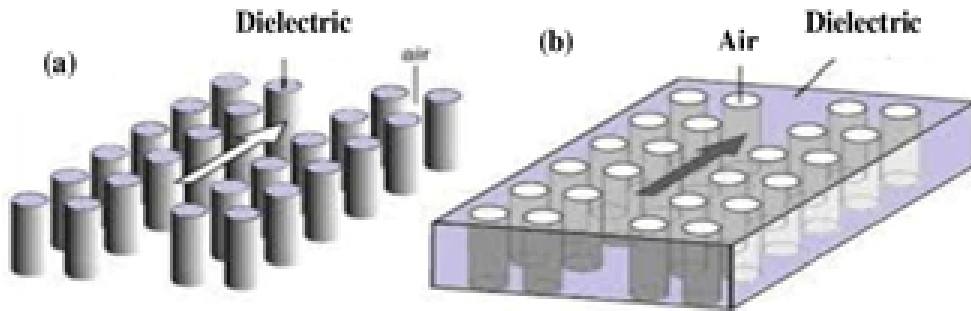


Figure 1.12: Diagram of a fault guide in a lattice (a) of rods of a dielectric (b) of air holes.

1.7 Cavities with photonic crystals

First study of microresonators carried out through passive one-dimensional guidance photonic structures proposed by Krauss et al, 1996 [30]. 1997 Foresi et al [31], and in 1997 Labilloy et al. two-dimensional crystals [32]. this The realization of cavities obtained by inclusion of point defects in crystals was born in 1998 [33]. In fact, we can roughly divide these voids into three categories Figure . These main types of cavities make it possible to obtain very high quality factors ($Q > 10^5$) at a low modal volume ($V < (\frac{\lambda}{n})^3$)

1.7.1 Point cavities

The cavities formed by the omission of one or more pores in the direction ΓK of the photonic crystal are generally called linear cavities and hexagonal cavities, represented respectively by L_n and H_h . An image with a scanning electron microscope (SEM) of an example of the L_3 cavity is presented in Figure 1.13 Subsequent studies have shown that the high quality factor of this type of cavity is due to the impedance matching at the edges of the cavity and to the slowing effect of the waves passing through the cavity [34] New modifications obtained by displacing the second and third holes adjacent to the cavity or by reducing their radii subsequently made it possible to obtain a quality factor of approximately 10^5 .

1.7.2 Hetero-structural cavities

Hetero-structural cavities were initially proposed by the S. Noda group in 2005 [35]. These structures are based on a progressive modulation of the period of the photonic crystal, which will form a potential well of the optical mode. Figure 1.14 The modification of the period of the photonic crystal acts locally on the crystal band structure, and the defects are found in the forbidden band. The periodic modulation is very low ($< 1\%$) and the transition between cavity and mirror will be very smooth, so few radiation modes will be introduced.

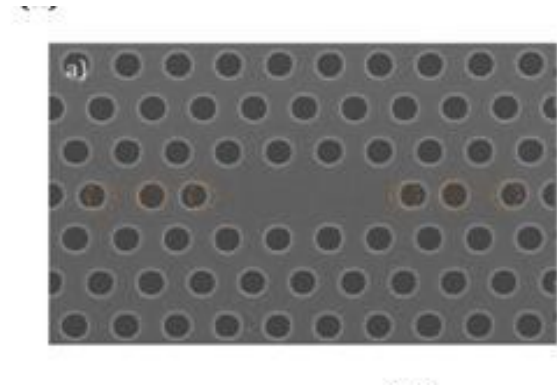


Figure 1.13: Scanning electron microscope (SEM) image of an L3-type cavity manufactured at the IEF.

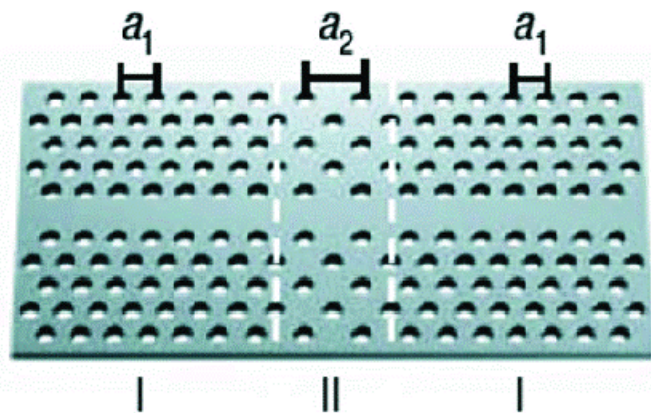


Figure 1.14: (a) Double hetero-structure cavity, made by connecting the basic structures with photonic crystals, I and II. The photonic crystal I has a triangular lattice structure with a lattice constant a_1 . The photonic crystal II has a triangular grating structure deformed into a rectangular grating with centered faces with a constant $a_2 (>a_1)$ in the direction of the waveguide. It has the same constant as that of the photonic crystal I in the orthogonal direction in order to satisfy the adaptation conditions of mesh.

1.8 Cavity structures with local modulation of linear defect width

Kuramochi initially proposed cavity structures with local modulation of linear defect width [36]. 800,000 silicon and 700,000 GaAs have been experimentally reached by the quality factor of this type of cavity [37]. This type of cavity is based on a linear defect in the photonic crystals of a network of triangular air holes, that is to say on a waveguide similar to a W1. The idea is to move the waveguide slightly away from a specific distance. Figure 1.15 schematically represents this structure.

The quality factor (Q) makes it possible to measure the ability of a resonator to conserve energy. The confinement of a mode at frequency ω_0 is determined by the loss rate of the cavity. Therefore, the quality factor Q of a resonant mode of frequency ω_0 is defined as the ratio of the energy stored in the resonator averaged over time to the energy dissipated

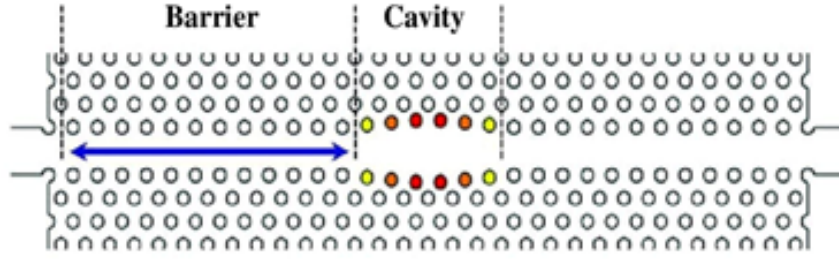


Figure 1.15: Diagram of an example of a cavity with linear defect width modulation. The displacement of the holes has been exaggeratedly increased for a better understanding.

per cycle, i.e. 1.4 :

$$Q = \frac{\text{stored energy}}{\text{energy dissipated per cycle}} = \omega_0 \frac{u}{p} \quad (1.4)$$

And the equation of The quality factor is given as the following form 1.5 :

$$Q = \frac{\omega_0}{\Delta\omega} = \frac{\lambda_0}{\Delta\lambda} \quad (1.5)$$

The quality factor and conditional size are two characteristic quantities of photonic crystal cavities. More precisely, the achievement of an optical cavity of a high-quality agent and a conditionally small size is necessary to facilitate the interaction of light substances.

1.9 Photonic crystal waveguide

Photonic crystal Wave guides first appeared in 1994 ,it is the creation of wave evidence by creating a linear defect in a photonic crystal .these guides are used to direct the propagation of light in a specific direction and are characterized by their small size, high efficiency and precise control over the propagation of light . Photonic crystal Wave guides are a promising technology for improving the efficiency and control of light propagation in various applications as ultra-sensitive sensors . Figure. 1.16

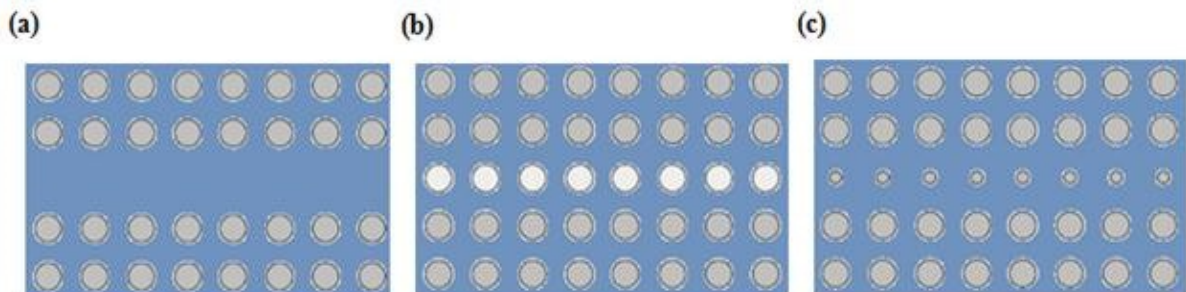


Figure 1.16: Examples of linear defects in a photonic crystal2 created (a) by omitting a single row of patterns, (b) by modifying the refractive index of a single row of patterns, (c) by varying the radius of a single row of patterns of the structure.

1.10 Guide/cavity coupling in a 2D photonic crystal

Research on 2D crystalline microcavities has shown that modes of quality factor greater than 1,000 can be obtained for cavities of a few microns. Photonic crystal conductors offer a natural way to connect these microcavities to planar optical circuits. Several coupling paths are possible Figure. 1.17 The first method consists in placing the cavity parallel to the guide to obtain a lateral interaction of the cavity mode with the guide mode. This coupling makes it possible to isolate one or more frequencies propagating in the guide. These frequencies can then be redirected, directly or not, to a second guide, also placed next to the cavity. Add-Drop wavelength applications are then possible. The second method consists in making a connection by the end of the guide by introducing a recess on the axis of the guide, a few patterns from its end. Most of the guided wavelengths will be reflected by this end, with the exception of a few which will be coupled to the cavity. This approach rather makes it possible to produce Fabry Perot type devices (if the second guide is directed towards the cavity).

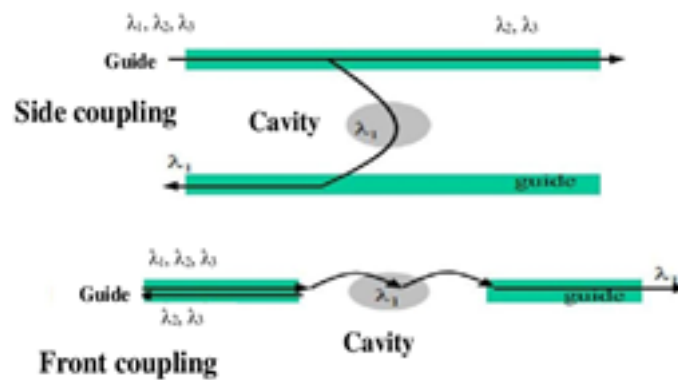


Figure 1.17: Passive and active devices associating guide and cavity of the same photonic crystal.

1.11 Applications of photonic crystals

Resonant cavities and optical crystal waveguides have been attracting great attention for about ten years because they provide new possibilities for creating ultrafine components for communications and optical sensors. In recent years, many devices have been proposed and studied in many areas, such as

Waveguides:

The PCs make it possible to create miniature and efficient waveguides for the transmission of light on the scale of the chip.

Couplers and Splitters:

PCs make it possible to couple and distribute light with great precision, which is crucial for integrated optical circuits.

Filters:

PCs can be used to create highly frequency-selective optical filters, allowing the spectrum of the transmitted light to be controlled.

Photonic Cavity Lasers:

PCs can be used to create miniaturized and high-performance photonic cavity lasers, with applications in optical communications and optical lithography.

PCs-based LEDs:

PCs can improve the efficiency and brightness of LEDs, which is important for lighting and display.

Pressure and Temperature Sensors:

PCs can be used to create highly sensitive pressure and temperature sensors based on changes in optical properties.

Biosensors:

The PCs can be integrated into biosensors for the sensitive and specific detection of biomolecules, with applications in medical diagnostics and environmental monitoring.

These new devices recreate the principles of operation of various components of integrated circuits, using photons as carriers of information instead of electrons.

1.12 Conclusion

Photonic crystals are one of the leading scientific innovations that have made a quantum leap in many technical and scientific fields. Thanks to their unique structure that enables them to accurately control the passage of electromagnetic waves, photonic crystals have become key tools in the development of advanced technologies, starting with optical communications. In this chapter, we provided basic information about photonic crystals, where we defined them and mentioned their natural and artificial types and the principles of each, then we touched on the characteristics of photonic crystals and various types of defects, mentioning the possibility of controlling photonic crystals in the propagation of light based on the band gap property (BGP). We have concluded this chapter with some of the applications on the basis of photonic crystals.

Chapter 2

Introduction to sensors based on photonic crystals

Contents

| | |
|---|-----------|
| 2.1 Introduction | 18 |
| 2.2 Definition | 18 |
| 2.3 Classification of sensors | 19 |
| 2.3.1 Active sensors | 19 |
| 2.3.2 Passive sensors | 19 |
| 2.4 Photonic crystal sensors | 20 |
| 2.5 Various types of sensors | 20 |
| 2.5.1 Physical sensor | 20 |
| 2.5.2 Chemical sensor | 21 |
| 2.5.3 Optical sensor | 21 |
| 2.6 Biosensor | 21 |
| 2.6.1 Operating Principle | 21 |
| 2.7 Different Types of Biosensors | 22 |
| 2.8 Basic characteristics of the biosensor | 22 |
| 2.8.1 Selectivity | 22 |
| 2.8.2 Reproducibility | 23 |
| 2.8.3 Stability | 23 |
| 2.8.4 sensitivity | 23 |
| 2.8.5 Linearity | 23 |
| 2.9 Optical biosensor | 24 |
| 2.9.1 Optical biosensors with photonic crystals | 24 |
| 2.10 Applications of Biosensors | 25 |
| 2.11 Conclusion | 25 |

2.1 Introduction

Sensors are devices that detect and respond to changes in their environment by producing an output signal. They are used in a wide range of applications, from monitoring temperature and pressure in industrial processes to detecting motion in security systems. Sensors can be found in everyday devices such as smartphones, cars, and home appliances, enabling them to interact with the world around them and provide valuable data for analysis and control. There are many different types of sensors, each designed to measure specific physical properties such as light, sound, temperature, motion, and more. Advances in sensor technology continue to drive innovation across various industries, making sensors an essential component of modern technology.

2.2 Definition

The sensor is the first episode of the measurement series. It acts as a power converter by interacting with a specific amount of material it wants to measure and characterize, and providing a usable amount of material, which must be measured, such as electrical voltage, frequency, intensity and deviation. External influencers such as temperature, humidity, chemical concentrations, etc. see Figure 2.1.

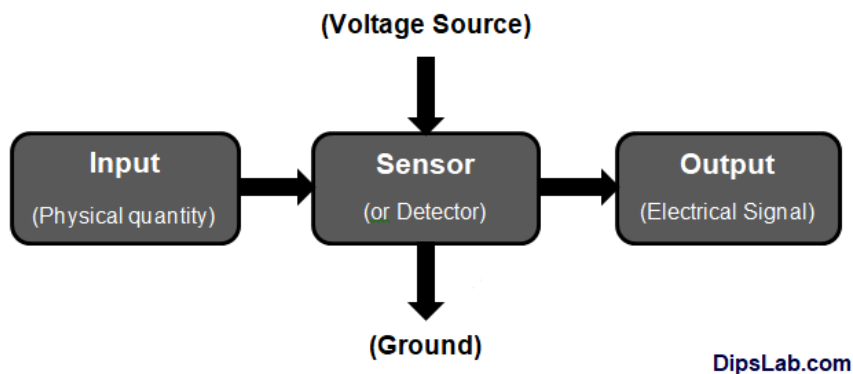


Figure 2.1: Principle of a sensor.

The different components of the sensor are described below. Figure 2.2 :

- Test body: element that selectively responds to the measured quantity. It transforms a measured quantity into another measurable physical quantity.
- Transducer: Converts the responses of the test body into an electrical quantity constituting an output signal.
- Transmitter: element that amplifies, filters and improves the output signal for remote transmission. It may or may not be integrated into the sensor.

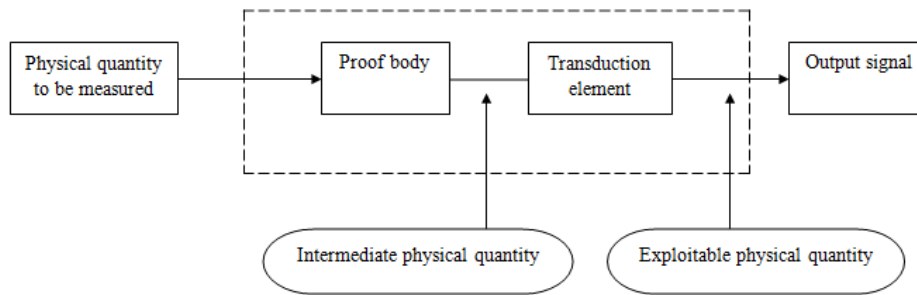


Figure 2.2: Constitution of a sensor.

2.3 Classification of sensors

The sensors are classified into two main families according to the characteristic electric of the output size :

2.3.1 Active sensors

A sensor is qualified as active when the physical phenomenon used to measure a quantity is converted directly into an electrical quantity. This conversion is governed by the same physical law which links the measurement to the quantity of electrical output. Often, active sensors act as electrical generators, producing an electrical potential difference at the output. Although the number of physical laws allowing this conversion is limited, the applications of active sensors are varied and extensive. [38]. The table 2.1.

Table 2.1: The effect used on the measurand to realize the output magnitude. [38].

| Measurand | EFFECT USED | Output quantity |
|-----------------|----------------------------------|-----------------|
| Temperature | Thermoelectricity (thermocouple) | tension, |
| Optical flow | Photoemission | Current |
| | Pyroelectric effect | Tension |
| | Photovoltaic effect | Tension |
| Power ,Pressure | Piezoelectricity | Electric charge |
| Position | Hall effect | Tension |
| Speed | electromagnetic induction | Tension |

2.3.2 Passive sensors

In most cases, passive sensors need external energy to function (as in the case of strain gauges, thermistors, etc.), they are often modeled by an impedance. A variation of the physical phenomenon studied (measured) generates a variation of the impedance. A voltage must be applied to obtain an output signal. The sensor behaves in output as a passive dipole that can be resistive, capacitive or inductive. Depending on the measurand, several effects are used to perform the measurement. The table 2.2 :

Table 2.2: Output Quantity Results by Selected Measures and Materials Used [39].

| Measurand | EFFECT USED (Output Size) | Materials |
|----------------------|-----------------------------|---|
| Temperature | Resistivity | Platinum, nickel, copper, |
| Very low temperature | Dielectric constant | semiconductors ,Glass |
| Optical flow | Resistivity | Semiconductors |
| Deformation | Resistivity Permeability | Nickel alloys, Ferromagnetic alloys |
| Position | Resistivity | Magnetoresistance: Bismuth, antimonyindium |
| Moisture | Resistivity | Lithium chloride |

2.4 Photonic crystal sensors

In the field of detection, sensors using PCs are a very promising area of research. The peculiarity of these crystals lies in their periodic structure, which makes it possible to capture photons and generate an optical Echo that is very sensitive to the presence of the molecules to be detected. In this way, they propose a variety of detection methods, which can be used in measurements ranging from air to highly volatile liquids [40]. Using the relationship between the optical properties of an photonic crystal and its physical and geometric properties, it is possible to distinguish different types of sensors [41]. These sensors include among others :

- Compression-based sensors use fluctuations in the refractive index of a photonic crystal to detect changes in the environment.
- Mechanical-optical sensors based on compression use the optical and mechanical properties of photonic crystals in order to measure physical elements such as pressure, force or deformation.
- Optical fiber sensors based on CPs: these sensors exploit optical fibers that integrate photonic crystals in order to determine parameters such as temperature, pressure or chemical concentration.

These different classes of sensors take advantage of the specific properties of photonic crystals in order to provide advanced detection capabilities in different sectors of use [17].

2.5 Various types of sensors

Each of the many types of sensors has a unique function and detection technology. The most common method is the transduction or the measurement of nature, whatever its use. Here are some examples of the different categories of sensors :

2.5.1 Physical sensor

A physical sensor is a device that measures a physical quantity, such as temperature, motion, light, mass and force ... etc. Physical sensors also work in different ways, using such physical principles as resistance, capacitance, inductance, optical conductivity. Data measured by physical sensors are often used to control systems and perform analyzes [42]

2.5.2 Chemical sensor

A chemical sensor is a device that analyzes and detects the concentration of chemical, biochemical, gaseous or liquid substances in general. It converts the concentration of a chemical species into an electrical signal while ensuring reproducibility, sensitivity and selectivity.

2.5.3 Optical sensor

An optical sensor is a device based on optical fibers or optical crystals with their high sensitivity, and various detection technologies related to these sensors are based on changes in information characterizing light waves [43].

2.6 Biosensor

An analytical device that transforms a biochemical phenomenon into a measurable signal is called a biosensor. It consists of a transducer and a biological component (called a bioreceptor). As shown in Figure 2.3 General principle of a biosensor.

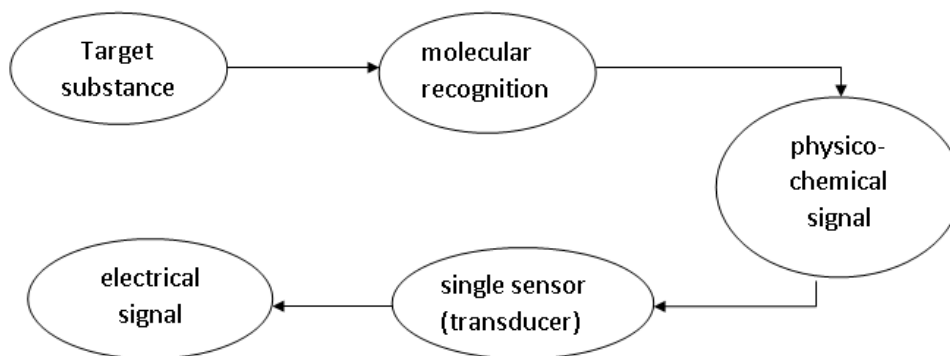


Figure 2.3: General principle of a biosensor

2.6.1 Operating Principle

A biosensor is a combination of a biological element, which can be an enzyme, an antibody, an antigen, a DNA fragment having a specific recognition function, and a transducer element, which can be an electrode, a quartz microbalance or an optical fiber, which ensures the transfer of a biological event "recognition of the analyzed element (analyte)" and its transformation into an exploitable signal (electrical or luminous). Presents the figure 2.4 Schematic diagram of biosensor comprising three components: detector, transducer and output system.

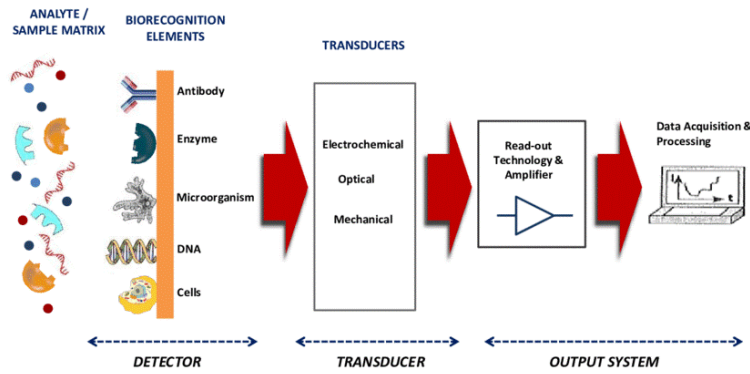


Figure 2.4: Schematic diagram of biosensor comprising three components: detector, transducer and output system.

2.7 Different Types of Biosensors

Biosensors are divided into two groups, that is, based on the biological component used in the analysis or the transduction method used. As mentioned earlier, some commonly used biological elements or elements of biological perception are DNA, enzymes, antibodies, tissues,... etc. The next and most widely used classification of biosensors is based on the type of transport used in the sensor, that is, the type of physical chemistry generated by the sensing event. Moreover, biosensors based on the mode of Transportation are again divided into three types. They are: Large-scale biological sensors Based on optical sensors Electrochemical sensors as shown in Figure 2.5 A diagram showing the different types of biosensors classified.

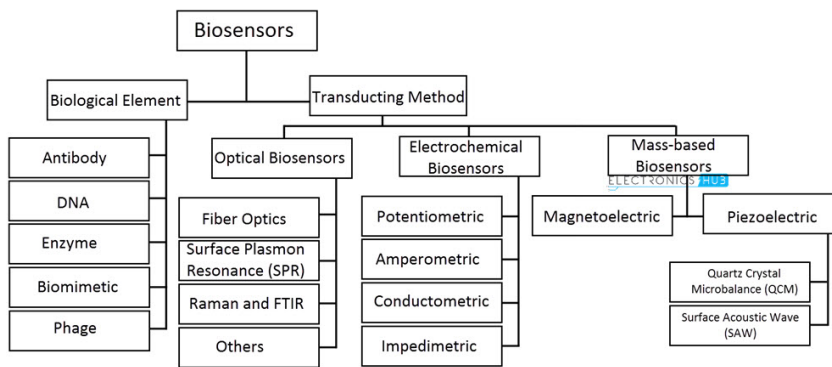


Figure 2.5: A diagram showing the different types of biosensors classified.

2.8 Basic characteristics of the biosensor

There are certain static and dynamic characteristics that every biosensor has. Optimization of these properties is reflected in the performance of the biosensor:

2.8.1 Selectivity

Selectivity is perhaps the most important advantage of a biosensor. Selectivity is the ability of a bioreceptor to detect a specific analytical substance in a sample containing

additives and other contaminants. When building a biosensor, the main factor taken into account when selecting a bioreceptor is selectivity.

2.8.2 Reproducibility

Reproducibility is the ability of a biosensor to generate identical responses for a duplicate experimental system. Repeatability is characterized by the precision and accuracy of the transducer and electronics in the biosensor. Precision is the ability of the sensor to provide identical results every time a sample is measured, and accuracy indicates the ability of the sensor to provide an average value close to the true value when the sample is measured more than once. Repeatable signals ensure high reliability and robustness of conclusions drawn from the biosensor response.

2.8.3 Stability

The biosensing system's stability refers to how susceptible it is to external perturbations both inside and outside of it. The output signals of a biosensor under measurement may wander as a result of these disruptions. This may result in a measurement mistake in the concentration and compromise the biosensors accuracy and precision. In situations when a biosensor needs to be continuously monitored or undergo lengthy incubation phases, stability is the most important characteristic.

2.8.4 sensitivity

The sensitivity or detection limit (DL) of a biosensor is defined as the lowest concentration of an analytical material that it can detect. in several applications for monitoring the environment and medicine. As a result, sensitivity is a crucial biosensor characteristic.

2.8.5 Linearity

Linearity is an attribute showing the accuracy of the measured response to a straight line, mathematically represented as 2.1:

$$y = m \times c \tag{2.1}$$

Where:

- c : the analyte concentration.
- y : the output signal.
- m : the sensitivity of the biosensor.

The linearity of a biosensor can be related to the resolution of the biosensor and the concentration range of the analyte being tested. Biosensor resolution is defined as the smallest change in analyte concentration required to cause a change in the biosensor response. Depending on the application, good resolution is required because most biosensor applications require not only detection of the analyte but also measurement of analyte concentrations over a wide operating range. Another term related to linearity is linear range, which is defined as the range of analyte concentrations for which the biosensor response varies linearly with concentration.

2.9 Optical biosensor

Optical biosensors are widely used in environmental, medical and biological research. Due to their sensitivity, selectivity and real-time analysis capability, they are useful in many applications. Here are some examples of optical biosensors that are frequently used:

2.9.1 Optical biosensors with photonic crystals

A type of optical biosensor that detects and analyzes biomolecular interactions using photonic crystals. The diagram of the optical detection system is illustrated in Figure 2.6 because photonic crystals are periodic structures that modify the properties of light when they pass through them. This is accomplished by measuring the change in the refractive index to detect analytes using the photonic crystal structure, as it provides a unique light confinement mechanism at the micro and nanoscale.

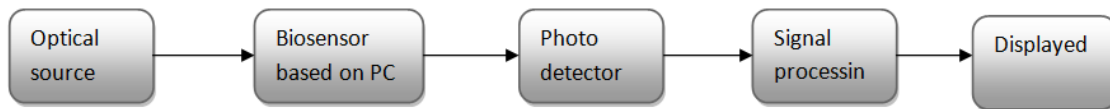


Figure 2.6: Schematic structure of optical detection system.

- **Biosensors based on waveguides coupled to the cavity**

These biosensors integrate in their design both a point defect (cavity) and a linear defect (waveguide). The type of cavity, whether it is a microcavity or a nanocavity, is determined according to the specifications of the designer and the analyte to be used. The waveguide structures combined with cavities allow optimal interaction between the light and the analytes, thus prolonging the lifetime of the photons inside the cavity. Therefore, this platform shows a high detection efficiency in biosensors.

- **Optical biosensors based on resonators**

Biosensors are based on resonators, which means that they incorporate a cavity, a waveguide and a ring in the center of the resonator. The configuration of the ring is influenced by the use of sensors and analytes, such as the round shape in elliptical resonator sensors. Biosensors are characterized by their exceptional sensitivity, high detection limit and high quality factor, which are their main characteristics. They also require a high transmission efficiency to detect a minimum number of analytes. Sometimes the sensor can have additional advantages when the analyte occupies a limited sensor detection area. Biosensors based on resonators are particularly advantageous for the detection of molecules in their own right. Biosensors that use resonators with a waveguide input and output to detect molecules of interest use these resonators. The use of biosensors allows the identification of targeted molecules in specific contexts, leading to innovative possibilities in fields as diverse as biomedical research and chemical detection.

2.10 Applications of Biosensors

Biosensors have become a crucial tool in medicine, clinical analysis and public health monitoring since their development in the early 1950s [44]. Biosensors offer significant advantages over laboratory equipment, including their small size, low cost, instant results, as well as ease of use. While biosensors are primarily used for medical and health monitoring, they have other practical uses in areas such as industrial processing, agriculture, food processing and pollution control ... etc.

Therefore, biosensors are commonly used in a limited number of possible applications, such as environmental monitoring, diagnostic applications, environmental monitoring, including industrial monitoring and food industry applications 2.7.

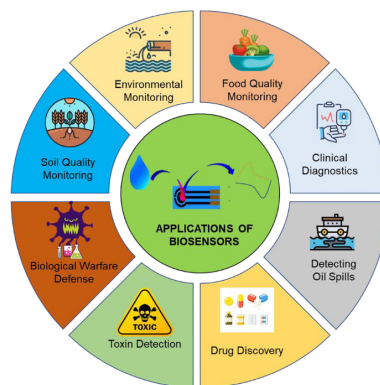


Figure 2.7: Applications of Biosensors.

2.11 Conclusion

Sensors are a key focus of modern technical and scientific developments, playing a vital role in a wide range of applications that include healthcare, industry, agriculture, and the environment. Thanks to its ability to convert physical and chemical phenomena into measurable electrical signals, the sensors enable accurate and effective monitoring and analysis of the surrounding environments. During this chapter, we covered key concepts about sensors and biosensors, where we first introduced sensors, their classification, various types and sensors based on photonic crystals. Secondly, we addressed biosensors by mentioning their characteristics and types of optical biosensors (waveform-based biosensors for detecting biological analytes, waveform-based biosensors paired with cavitation). We ended the chapter with the areas of application of biosensors.

Chapter 3

Design of a PC-2D based biosensor for the detection of blood components

Contents

| | |
|--|----|
| 3.1 Introduction | 27 |
| 3.2 Performance parameters | 27 |
| 3.3 The mechanism of action of PCs sensor for the detection of biomolecules | 28 |
| 3.4 PC-2D hexagonal lattice structure | 28 |
| 3.5 Photonic bandgap analysis | 29 |
| 3.6 Design of a PC biosensor based on a cavity coupled to a waveguide . . . | 29 |
| 3.7 Distribution of the electric field | 30 |
| 3.8 Transmission spectrum of the biosensor | 31 |
| 3.9 How biomolecules attach to measuring rods | 31 |
| 3.10 Simulation results | 32 |
| 3.11 Conclusion | 37 |

3.1 Introduction

We studied and improved the biosensor after the studies conducted on optical crystals in biosensors. So, in this chapter, we will present the structure to be analyzed based on two-dimensional optical crystals. After that, we will propose a structure consisting of a cavity and a waveguide at the structure level and then measure the quality of the sensor and wavelength transition. The purpose of this study is to detect brain lesions. The RSoft CAD simulator program was used to study this project using the PWE and FDTD methods. This software is specialized in the creation and analysis of photonic crystal structures.

3.2 Performance parameters

The study of the performance of the biosensor is based on the use of the time domain method of finite difference 2 D (FDTD).

The quality factor (Q) is the most crucial characteristic in Biosensors based on PCs, which is indicated in the following way 3.1 [45] [46]:

$$Q = \frac{\lambda_0}{\Delta\lambda_{FWHM}} \quad (3.1)$$

The central resonance wavelength is λ_0 while the spectral width at mid-height for the central transmission spectrum is $\Delta\lambda$.

The sensitivity of the biosensors is another crucial element. The sensitivity level corresponds to the degree of modification of the transmission of a signal to a biosensor in response to a modification of the connection of an analyte in a detection rod. It is provided by the formulation 3.2 [45] [46]:

$$S = \frac{\Delta\lambda}{\Delta n} \quad (3.2)$$

The shift of the position of the transmission spectrum produced by the studied biosensor is represented by $\Delta\lambda$ and Δn corresponds to the change in the refractive index.

The detection limit is another essential parameter, which is represented by the equation 3.3 [47] [48]:

$$DL = \frac{\lambda_0}{10 \times S \times Q} \quad (3.3)$$

The sensitivity and the quality factor are represented by S and Q, respectively.

The merit factor (FOM) is the next parameter, calculated as follows 3.4 [49]:

$$FOM = \frac{Q \times S}{\lambda_0} \quad (3.4)$$

3.3 The mechanism of action of PCs sensor for the detection of biomolecules

Photonic crystals biosensors (PCs) are a new technology for detecting biomolecules with incomparable precision and sensitivity. These sensors use the interaction between the target biomolecule and a specific recognition element fixed on the surface of the PC. This interaction leads to a change in the optical characteristics of the PC, which can be detected using advanced optical techniques. PCs biosensors offer multiple benefits compared to conventional detection techniques, such as their high sensitivity, high specificity, reusability, and miniaturization. These characteristics are advantageous for many applications, such as early cancer diagnosis, infectious disease detection, health monitoring, food safety, and water monitoring.

3.4 PC-2D hexagonal lattice structure

We used a hexagonal lattice of 2D photonic crystals consisting of 15×15 circular rods along the X and Z axes, respectively, in our project. The structure will be elaborated using silicon rods (Si) with a refractive index of 3.46000 RIU placed in the air background with an n air refractive index of 1 RIU, with a period of 600 nm and a radius of rods of 120 nm. The geometric diagram of the 15×15 hexagonal structure based on 2D photonic crystals is presented in the figure 3.1. The table 3.1 presents the parameters of interest used in the simulation.

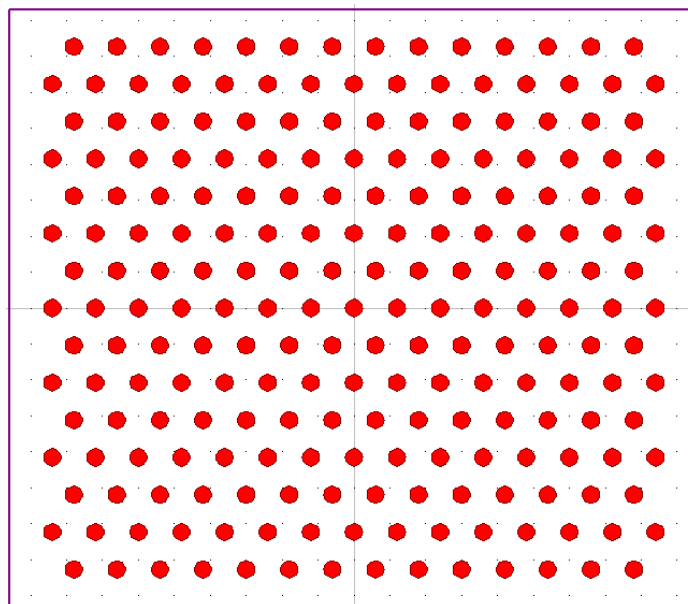


Figure 3.1: The diagram of the hexagonal structure used for the biosensor design is based on 2D-PCs.

Table 3.1: Optical and geometric parameters of the hexagonal structure based on PCs.

| Parameters | Values |
|--|-----------------------|
| Lattice | Hexagonal |
| Shape of the rods | Circles |
| Dimensions of the platform | (15x15 rods) |
| Radius of the rod (r) | 120 nm |
| Lattice constant (a) | 600 nm |
| Refractive index of the background (Air) | 1 |
| Refractive index of rods (Si) | 3.46 |
| Size | 72.59 μm^2 |

3.5 Photonic bandgap analysis

Figure 3.2, Shows a light band gap diagram calculated using the plane wave method. We use a Gaussian-type range to determine the TE polarization scheme, where we obtain two bands; the first band is located between the frequencies 0.27605 and 0.44544 and its wavelength ranges between 1326.98 nm and 2173.51 nm, which corresponds to the second and third optical transmission windows (1550 nm and 1300 nm), the second band is located between the frequencies 0.59392 and 0.56255 and its wavelength ranges between 1010 nm and 1066 nm it is not compatible with any of the optical transmission windows.

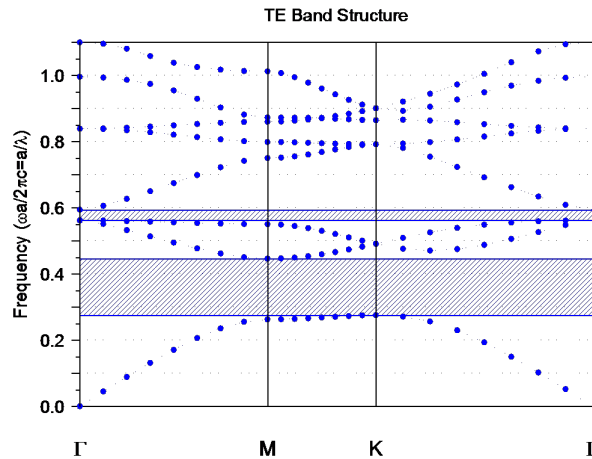


Figure 3.2: Presents a diagram of photonic bandgaps of the hexagonal grating structure in PC.

3.6 Design of a PC biosensor based on a cavity coupled to a waveguide

It is essential to have input and output channels to design a biosensor that uses a two-dimensional photonic crystal structure to manufacture linear defects and cavities. Next, create a hexagonal cavity using a waveguide below and above the cavity in parallel, as shown in figure 3.3.

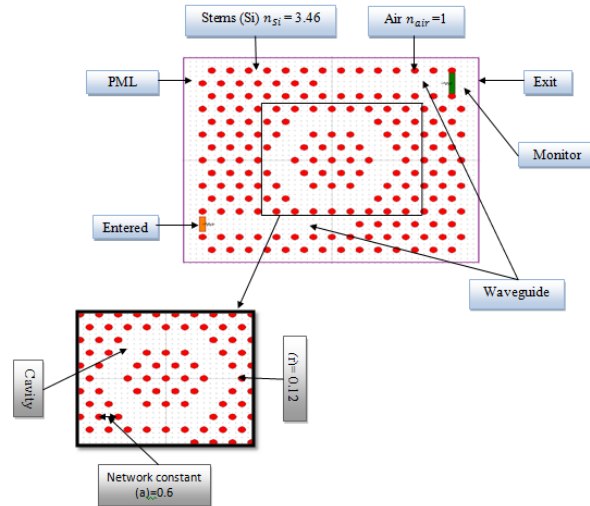


Figure 3.3: Biosensor structure designed with a cavity.

3.7 Distribution of the electric field

Using the FDTD method and the type of excitation of the default launch (CW) with the choice of the TE polarization for the analysis of the structure designed for the biosensor, the results obtained are presented in figure 3.4 which shows the distribution of the electric field in the cavity of our proposed device. It is observed that the light propagates in the waveguide and the cavity, with a small loss of light outside the waveguide.

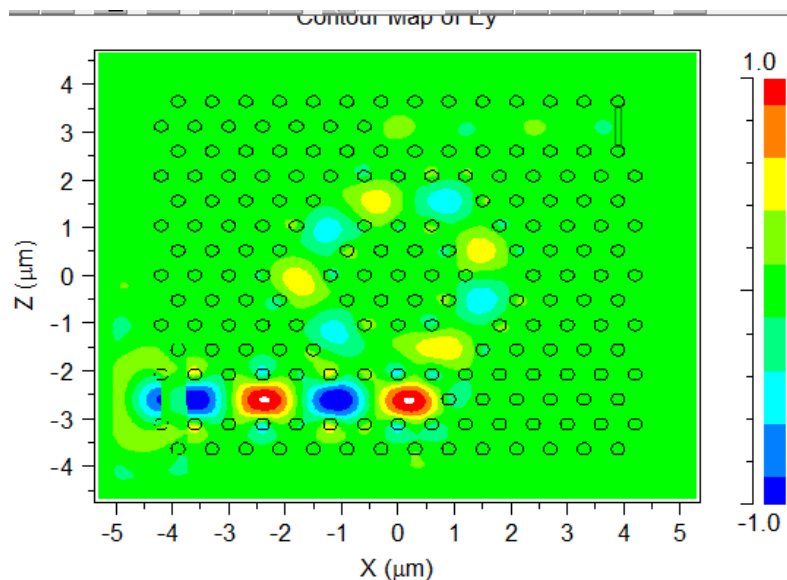


Figure 3.4: Distribution of the electric field in 2D of biosensor based with on a resonant cavity (b) frequency-denoted biosensor transmission spectrum (c) the transmission spectrum of biosensor in terms of the resonance wavelength.

3.8 Transmission spectrum of the biosensor

Figure 3.5 represents the transmission spectrum of the biosensor in terms of resonance wavelength. The normal transmission spectrum of the biosensor is shown in the absence of biomolecules, with the choice of the type of excitation of the default release (Pulsed) and the TE polarization. The resonance wavelength is 1408.4 nm and the transmission power is equivalent to 76%.

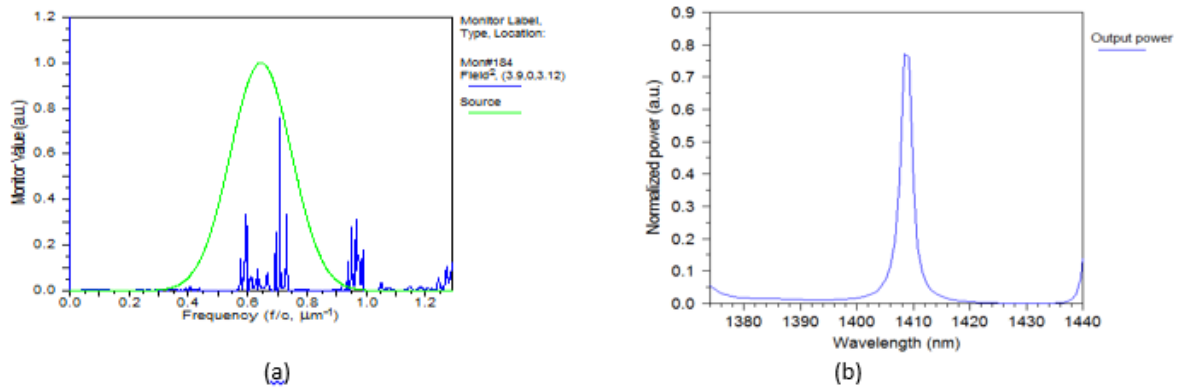


Figure 3.5: (a) frequency-denoted biosensor transmission spectrum (b) the transmission spectrum of biosensor in terms of the resonance wavelength.

3.9 How biomolecules attach to measuring rods

Photonic crystal biosensors take advantage of refractive index differences to detect specific molecules. When particles are attached to the measuring rods of the photonic crystals, changes in the local refractive index occur, which lead to wavelength adjustments and, consequently, fluctuations in the position of the maximum intensity. The refractive index plays a leading role in this process because it measures the speed of light in a material relative to its speed in a vacuum. In a photonic crystal, this indicator depends on the order of the structure and the optical properties of the materials used in its manufacture. In our work, the material in question is silicone. When the surface of the biosensor structure is affected by light, this light passes through the different layers of the crystal structure. At each transition between the layers, the light is subjected to reflection phenomena, which generate constructive and destructive interferences, resulting in the appearance of interference fringes. The wavelength of the photonic crystals corresponds to the wavelength at which the interference occurs as constructive as possible, improving the reflection of light. After the molecules are attached to the crystal surface, the resonance wavelength of the crystal is also changed due to the adjustment of the refractive index. This variability can be measured to detect the presence of target molecules. Once the biomolecules have been selected and attached to the surface of the photonic crystal, the biosensor is ready to continue the process of their detection. To simulate a biosensor, we selected measuring rods, as shown in the figure 3.6 the excitation type of the default launch (pulsed) with the choice of TE polarization.

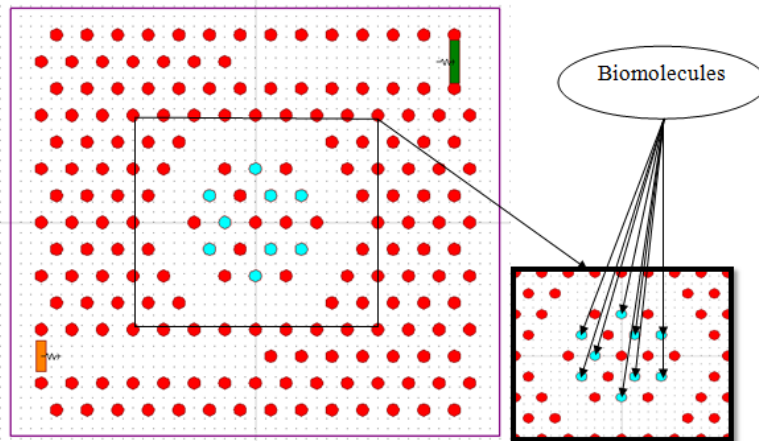


Figure 3.6: Biosensor structure designed with a cavity and biomolecules

3.10 Simulation results

Figure 3.7 presents the output of the sensor is observed without the presence of a biomolecule. In the reference mode, the resonance wavelength is 1528.4 nm, and the transmission power is 0.83 (a.u) with a refractive index of 1 RIU. The quality factor in this mode is 849.111.

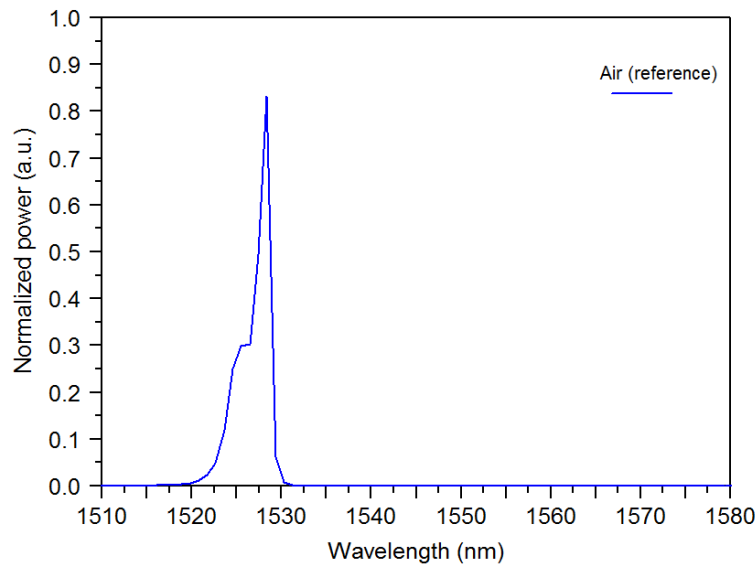


Figure 3.7: Biosensor output in reference mode (air).

In figure 3.8 ,we observe the sensor output after adding Water particles shifted by the resonance wavelength value of 1546.6 nm and the transmission power of 0.67 (a.u) with a refractive index of 1.33 RIU.In addition, the quality factor is 533.31 and the sensitivity is 55.15 nm/RIU.

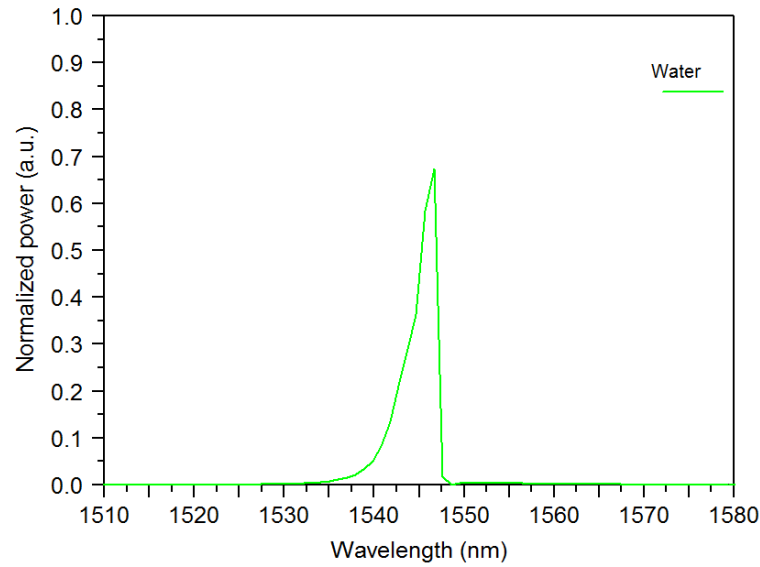


Figure 3.8: Biosensor output for Water.

The figure 3.9 illustrated the output of the sensor after the addition of Blood plasma particles shifted by the resonance wavelength value of 1547.6 nm and the transmission power of 0.95(a.u) with a refractive index of 1.35 RIU. In addition, the quality factor is 1190.46 and the sensitivity is 54.8 nm/RIU.

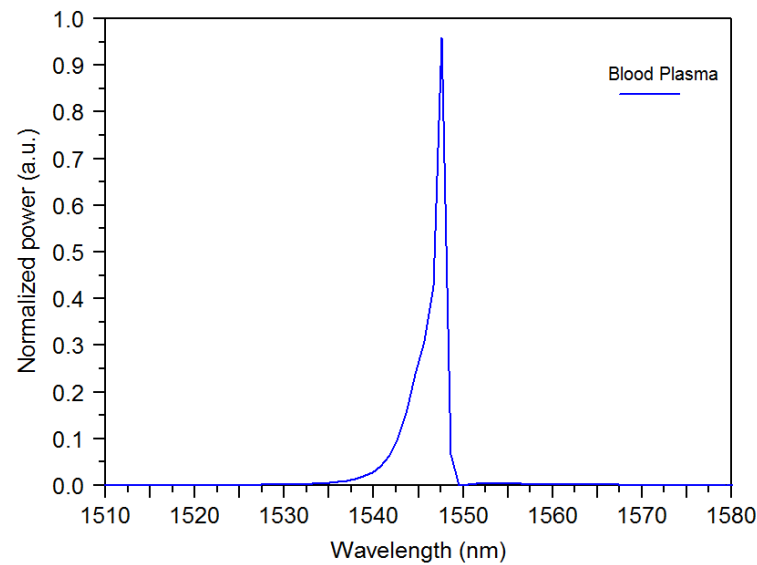


Figure 3.9: Biosensor output for Blood Plasma.

Figure 3.10 depicted the sensor output after adding Ethanol particles shifted by the resonance wavelength value of 1548.5 nm and the transmission power of 0.74 (a.u) with a refractive index of 1.36 RIU. In addition, the quality factor is 619.4 and the sensitivity is 55.83 nm/RIU.

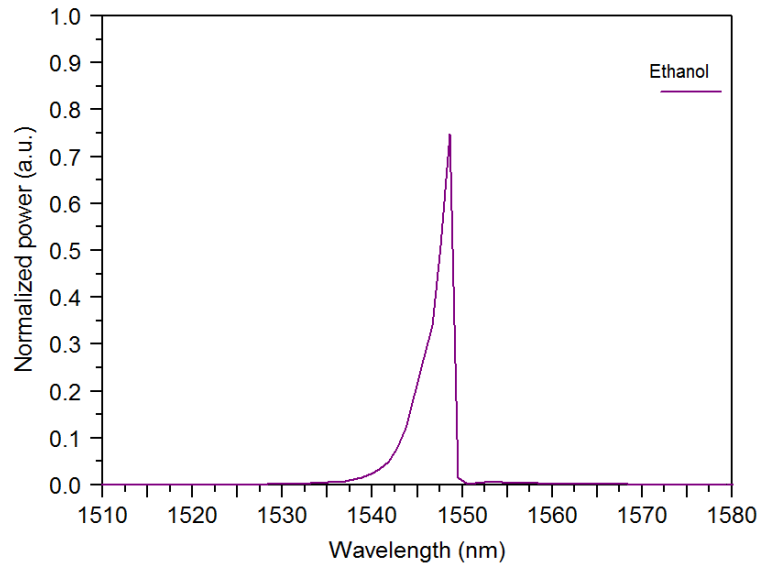


Figure 3.10: Biosensor output for Ethanol.

In figure 3.11, we observe the sensor output after the addition of Sylgard184-Glucose particles shifted by the resonance wavelength value of 1551.8 nm and the transmission power of 0.56 (a.u) with a refractive index of 1.4 RIU. In addition, the quality factor is 484.93 and the sensitivity is 58.5 nm/UIR.

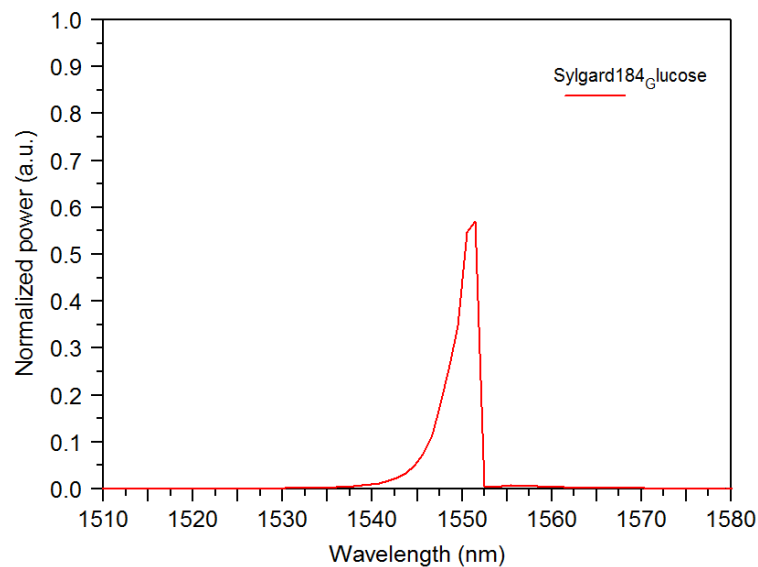


Figure 3.11: Biosensor output for Sylgard184-Glucose.

As shown in figure 3.12, after adding Polyacrylamide particles, we observed that the sensor output is shifted by the resonance wavelength value of 1554.5 nm and the transmission power of 0.51 (a.u) with a refractive index of 1.452 RIU. In addition, the quality factor is 485.78 and the sensitivity is 57.74 nm/RIU.

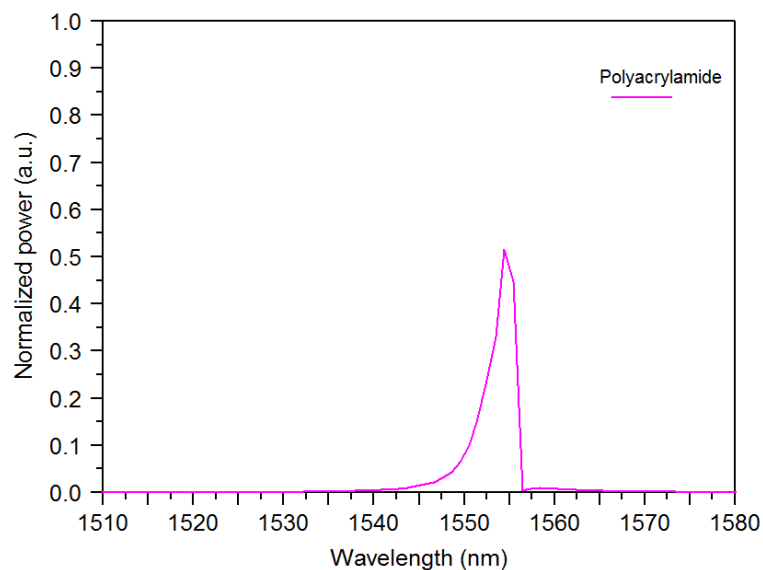


Figure 3.12: Biosensor output for Polyacrylamide.

In figure 3.13, we observed that the sensor output after adding Bovine-Serum-Albumin particles is shifted by the resonance wavelength value of 1556.3 nm and the transmission power of 0.77 (a.u) with a refractive index of 1.47 RIU. In addition, the quality factor is 1037.53 and the sensitivity is 59.36 nm/RIU.

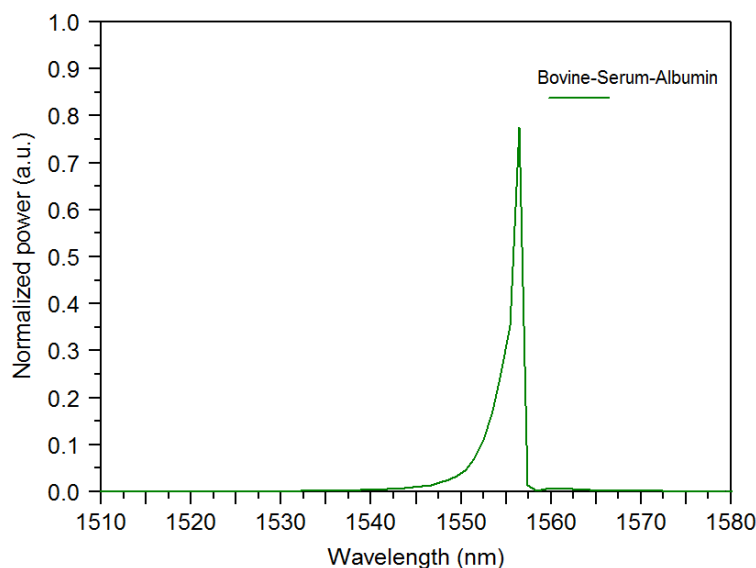


Figure 3.13: Biosensor output for Bovine-Serum-Albumin.

In figure 3.14, we observe the sensor output after adding Urethane-Dimethacrylate particles shifted by the resonance wavelength value of 1557.6 nm and the transmission power of 0.69 (a.u) with a refractive index of 1.481 RIU. In addition, the quality factor is 916.23 and the sensitivity is 60.70 nm/RIU.

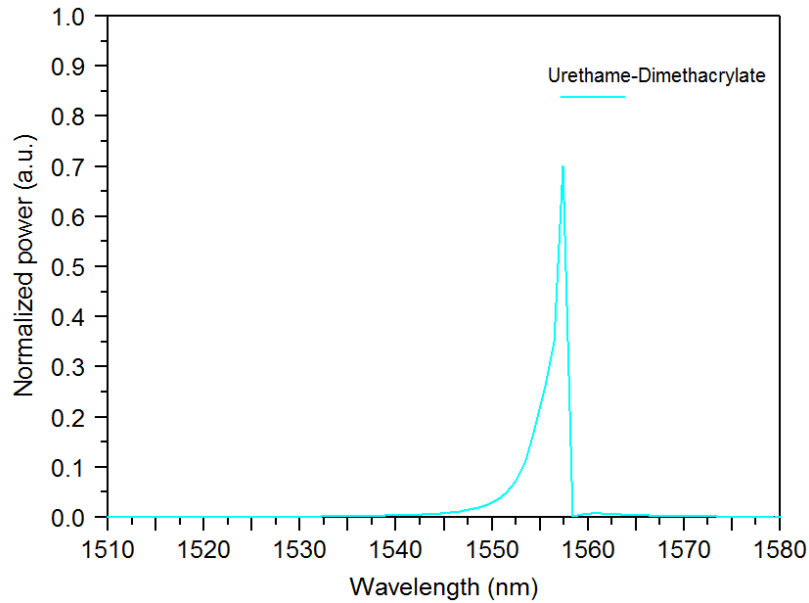


Figure 3.14: Biosensor output for Urethane-Dimethacrylate.

Figure 3.15, Shows the output spectra of a biosensor of blood components. The results are presented by changing the refractive indices from 1.33 RIU to 1.481 RIU.

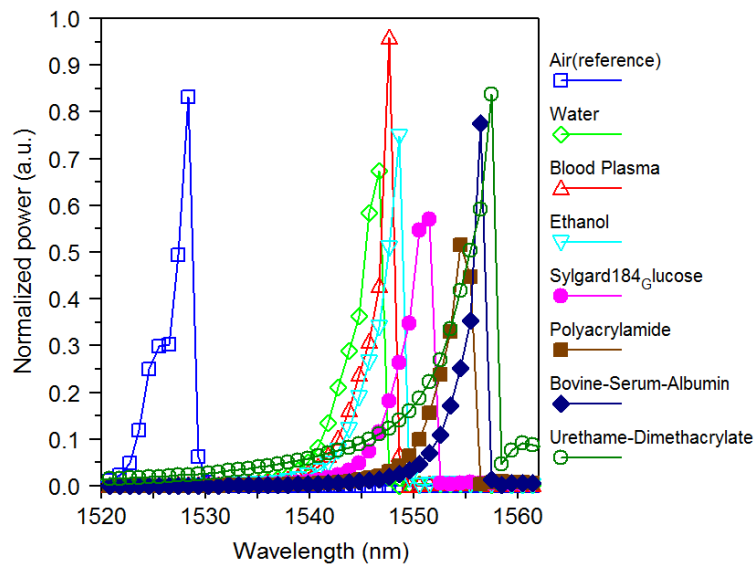


Figure 3.15: The resonance wavelength spectra produced at various blood components with refractive indices.

Table 3.2, Summarizes the results obtained by the biosensor during the connection of refractive indices of blood components to the measuring rods located in the cavity. Parameters such as detection limit, FOM, quality factor, and sensitivity are also included in this table to describe the structure's performance. We note that there is a relationship between the quality factor, sensitivity and FOM; when the quality factor and sensitivity increase, the FOM value also increases, and the maximum value of the FOM obtained was $42.197 \text{ (RIU)}^{-1}$, with a sensitivity of 54.857 nm / RIU and a quality factor of 1190.461, this value represents the highest performance we received, with a low detection limit of 0.0023. On the other hand, the minimum FOM value was $18.044 \text{ (RIU)}^{-1}$, with a sensitivity of 57.743

nm/RIU and a quality factor of 485.781, this value represents the lowest performance we have obtained. The most significant value obtained from DL is 0.0554 RIU.

Table 3.2: Sensor output according to biomolecules connected to the measuring rods.

| Name | RI | $\Delta\lambda_{FWHM}$ | λ | Q | S | LD | FOM |
|-------------------------|-------|------------------------|-----------|---------|-------|--------|-------|
| Reference (Air) | 1 | 1.8 | 1528.4 | 849.11 | - | - | - |
| Water | 1.33 | 2.9 | 1546.6 | 533.31 | 55.15 | 0.0052 | 19.01 |
| Blood Plasma | 1.35 | 1.3 | 1547.6 | 1190.46 | 54.85 | 0.0023 | 42.19 |
| Ethanol | 1.36 | 2.5 | 1548.5 | 619.40 | 55.83 | 0.0044 | 22.33 |
| Sylgard184-Glucose | 1.4 | 3.2 | 1551.8 | 484.93 | 58.50 | 0.0547 | 18.28 |
| Polyacrylamide | 1.452 | 3.2 | 1554.5 | 485.78 | 57.74 | 0.0554 | 18.04 |
| Bovine-Serum-Albumin | 1.47 | 1.5 | 1556.3 | 1037.53 | 59.36 | 0.0025 | 39.57 |
| Urethane-Dimethacrylate | 1.481 | 1.7 | 1557.6 | 916.23 | 60.70 | 0.0028 | 35.29 |

-1. RI= Refractive index (RIU) -2. $\Delta\lambda_{FWHM}$ =the displacement of the transmission spectrum (nm)-3. λ = Resonance wavelength (nm) -4. Q=Quality factor -5. S=Sensitivity (nm/RIU) -6. DL=Detection limit (RIU) -7. FOM=Merit factor (RIU)⁻¹

3.11 Conclusion

This chapter presents a proposed biosensor structure with two-dimensional photonic crystals using silicon rods in the background of an air-based waveguide coupled to a single cavity. We have introduced the principle of opening the photonic band gaps and a band map, which makes it possible to determine the parameters of the photonic crystal lattice. The hexagonal mesh parameters are carefully selected to open a wide band gap and obtain a wide detection range of the biosensor in a frequency range corresponding to the third communication window. The introduction of a linear defect in the studied two-dimensional photonic crystal ensures the confinement of light in one dimension and its propagation in the other, which forms a waveguide that makes it possible to process all the information. We used PWE and FDTD methods to study all functional aspects of our proposed biosensors. The study of the detection of blood components has achieved impressive results with the best quality factor of 1190.461; it guarantees optimal accuracy and reliability in the analysis of blood components, the sensitivity reaches 60.706 nm/RIU, and the maximum Detection limit of 0.0554 RIU in addition, the FOM wall factor, which assigns the efficiency and overall performance of the system is between 42.197(RIU)⁻¹. All These results were obtained at wavelengths of about 1528.4 nm and 1557.6 nm.

Chapter 4

Optimization of the sensitivity of the PC biosensor by varying the number of measuring rods

Contents

| | |
|---|-----------|
| 4.1 Introduction | 39 |
| 4.2 Optimization of the biosensor based on photonic crystals by the number of measuring rods | 39 |
| 4.2.1 Case1: Number of rods connected to the biomolecules is 9 rods . . . | 39 |
| 4.2.2 Case2: Number of rods connected to the biomolecules is 12 rods . . | 40 |
| 4.2.3 Case3: Number of rods connected to the biomolecules is 18 rods . . | 42 |
| 4.2.4 Case4: Number of rods connected to the biomolecules is 54 rods . . | 43 |
| 4.3 Comparison of the proposed biosensor with different designs with PCs bases | 47 |
| 4.4 Conclusion | 47 |

4.1 Introduction

Biosensors are effectively used in many applications to detect parameters such as hematology and cancer, which is very important and used in medical diagnostics. We have provided a structure for a biosensor based on PCs-2D to determine the resonance wavelength and obtain a higher sensitivity and a good quality factor. In this chapter, we used the same structure as the previous one with a change of measuring rods. The simulation results were obtained with the RSOFTE program using the FDTD and PWE methods.

4.2 Optimization of the biosensor based on photonic crystals by the number of measuring rods

4.2.1 Case1: Number of rods connected to the biomolecules is 9 rods

In this case, we selected 9 measuring rods as biomolecules to study the performance of the photonic biosensor, as shown in figure 4.1 .In figure 4.2 shows the output spectra of the biosensor of measuring rods 9.

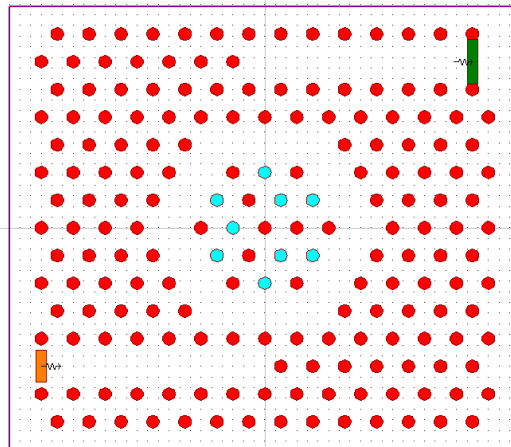


Figure 4.1: The structure of the biosensor for 9 measuring rods.

Table 4.1 presents the simulation results showing that the maximum value of the FOM obtained was $42.197 \text{ (RIU)}^{-1}$, with a sensitivity of 54.857 nm/RIU and a quality factor of 1190.461. This value represents our highest performance, with a refractive index of 1.35 RIU. On the other hand, the minimum value of the FOM was $18.044 \text{ (RIU)}^{-1}$, with a sensitivity of 57.743 nm/RIU and a quality factor of 485.781. This value represents our lowest performance, with a refractive index of 1.452 RIU. The maximum DL value obtained was 0.0554 RIU, with the same sensitivity and previous quality factor, for a wavelength of 1554.5nm.

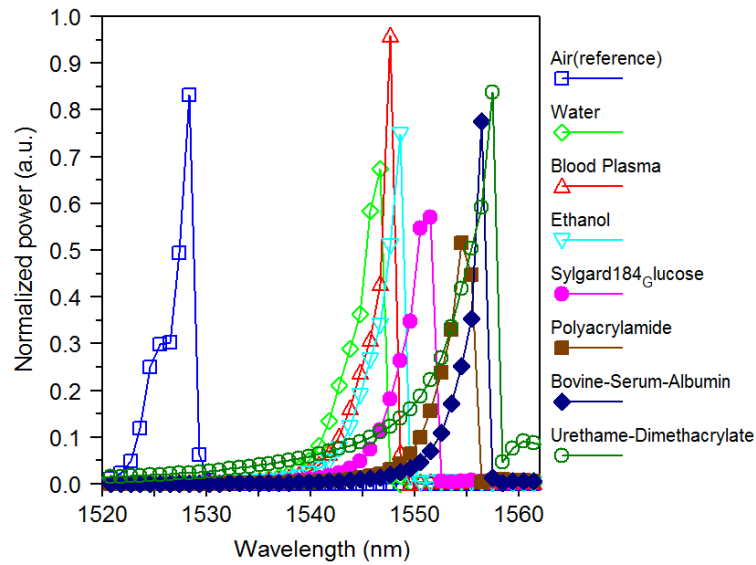


Figure 4.2: The transmission spectra of the biosensor for 9 functional rods.

Table 4.1: Summarizes the results obtained by the biosensor during the conduction of refractive indices of blood components in the case of N=9.

| Name | RI | $\Delta\lambda_{FWHM}$ | λ | Q | S | LD | FOM |
|-------------------------|-------|------------------------|-----------|---------|-------|--------|-------|
| Reference (Air) | 1 | 1.8 | 1528.4 | 849.11 | - | - | - |
| Water | 1.33 | 2.9 | 1546.6 | 533.31 | 55.15 | 0.0052 | 19.01 |
| Blood Plasma | 1.35 | 1.3 | 1547.6 | 1190.46 | 54.85 | 0.0023 | 42.19 |
| Ethanol | 1.36 | 2.5 | 1548.5 | 619.40 | 55.83 | 0.0044 | 22.33 |
| Sylgard184-Glucose | 1.4 | 3.2 | 1551.8 | 484.93 | 58.50 | 0.0547 | 18.28 |
| Polyacrylamide | 1.452 | 3.2 | 1554.5 | 485.78 | 57.74 | 0.0554 | 18.04 |
| Bovine-Serum-Albumin | 1.47 | 1.5 | 1556.3 | 1037.53 | 59.36 | 0.0025 | 39.57 |
| Urethane-Dimethacrylate | 1.481 | 1.7 | 1557.6 | 916.23 | 60.70 | 0.0028 | 35.29 |

-1.RI= Refractive index (RIU) -2. $\Delta\lambda_{FWHM}$ =the displacement of the transmission spectrum (nm)-3.
 λ =Resonance wavelength (nm) -4.Q=Quality factor -5. S=Sensitivity (nm/RIU) -6. DL=Detection limit (RIU) -7. FOM=Merit factor(RIU)⁻¹

4.2.2 Case2: Number of rods connected to the biomolecules is 12 rods

In this case, we selected 12 measuring rods as biomolecules to study the performance of the photonic biosensor, as shown in figure 4.3. In figure 4.4 shows the output spectra of the biosensor of measuring rods 12.

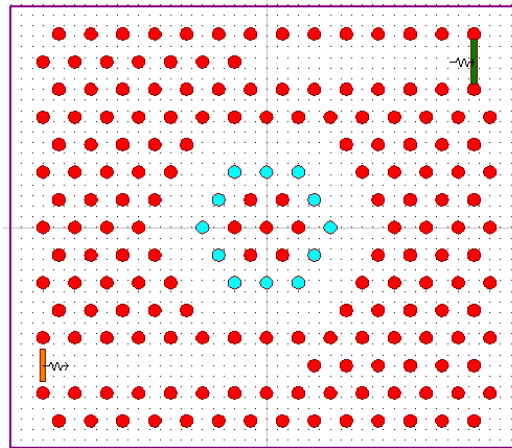


Figure 4.3: The structure of the biosensor for 12 measuring rods.

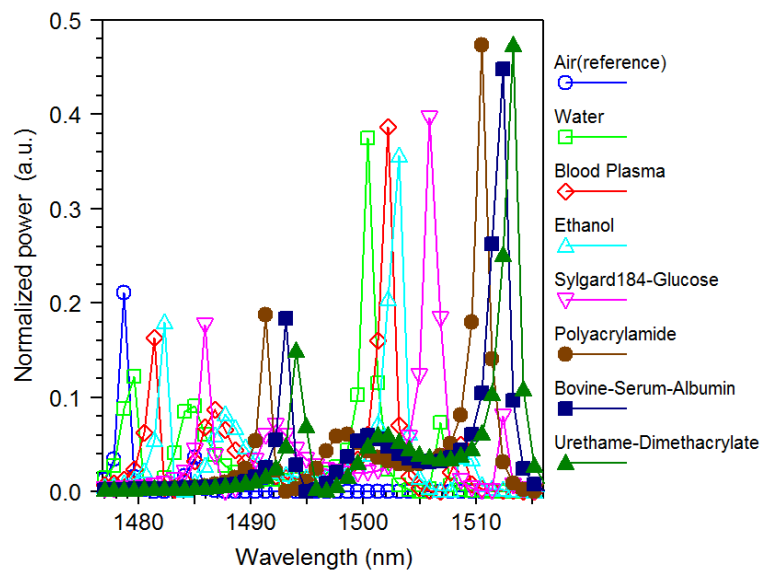


Figure 4.4: The transmission spectra of the biosensor for 12 functional rods.

The table 4.2 presents the simulation results showing that the maximum value of the FOM obtained was 50.57 (RIU)^{-1} , with a sensitivity of 65.75 nm/RIU and a quality factor of 1154.15. This value represents our highest performance, with a refractive index of 1.33 RIU. On the other hand, the minimum value of the FOM was 39.83 (RIU)^{-1} , with a sensitivity of 71.70 nm/RIU and a quality factor of 840.22. This value represents our lowest performance, with a refractive index of 1.47 RIU. The maximum DL value obtained was 0.00251 RUI, with the same sensitivity and the same previous quality factor for a wavelength of 1512.4 nm.

Table 4.2: Summarizes the results obtained by the biosensor during the conduction of refractive indices of blood components in the case of N=12.

| Name | RI | $\Delta\lambda_{FWHM}$ | λ | Q | S | LD | FOM |
|-------------------------|-------|------------------------|-----------|---------|-------|---------|-------|
| Reference (Air) | 1 | 1 | 1478.7 | 1478.70 | - | - | - |
| Water | 1.33 | 1.3 | 1500.4 | 1154.15 | 65.75 | 0.00197 | 50.57 |
| Blood Plasma | 1.35 | 1.4 | 1502.2 | 1073 | 67.14 | 0.00208 | 47.95 |
| Ethanol | 1.36 | 1.7 | 1503.1 | 884.17 | 67.77 | 0.00250 | 39.86 |
| Sylgard184-Glucose | 1.4 | 1.6 | 1505.9 | 941.18 | 68 | 0.00235 | 42.49 |
| Polyacrylamide | 1.452 | 1.4 | 1510.5 | 1078.92 | 70.35 | 0.00199 | 50.24 |
| Bovine-Serum-Albumin | 1.47 | 1.8 | 1512.4 | 840.22 | 71.70 | 0.00251 | 39.83 |
| Urethane-Dimethacrylate | 1.481 | 1.6 | 1513.3 | 945.81 | 71.93 | 0.0022 | 44.95 |

-1.RI= Refractive index (RIU) -2. $\Delta\lambda_{FWHM}$ =the displacement of the transmission spectrum (nm)-3.
 λ =Resonance wavelength (nm)-4.Q=Quality factor -5. S=Sensitivity (nm/RIU) -6. DL=Detection limit (RIU)
 -7. FOM=Merit factor (RIU)⁻¹

4.2.3 Case3: Number of rods connected to the biomolecules is 18 rods

In this case, we selected 18 measuring rods as biomolecules to study the performance of the photonic biosensor, as shown in figure 4.5. In figure 4.6 shows the output spectra of the biosensor of measuring rods 18.

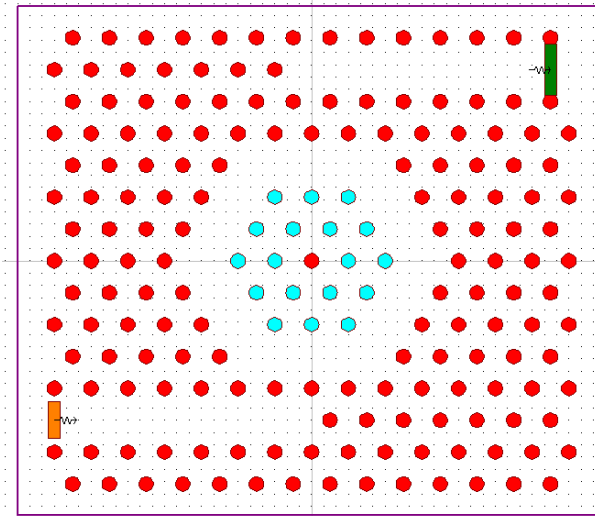


Figure 4.5: The structure of the biosensor for 18 measuring rods.

The table 4.3 presents the simulation results showing that the maximum value of the FOM obtained was $65.141 \text{ (RIU)}^{-1}$, with a sensitivity of 78.170 nm/RIU and a quality factor of 1236.833 . This value represents our highest performance, with a refractive index of 1.481 RIU . On the other hand, the minimum value of the FOM was $32.322 \text{ (RIU)}^{-1}$, with a sensitivity of 67.878 nm/RIU and a quality factor of 699.523 . This value represents the lowest performance we have obtained, with a refractive index of 1.33 RIU . The maximum value of DL obtained was 0.0030 RIU , with a sensitivity of 67.878 nm/RIU and a quality factor of 699.523 , for a wavelength of 1469 nm .

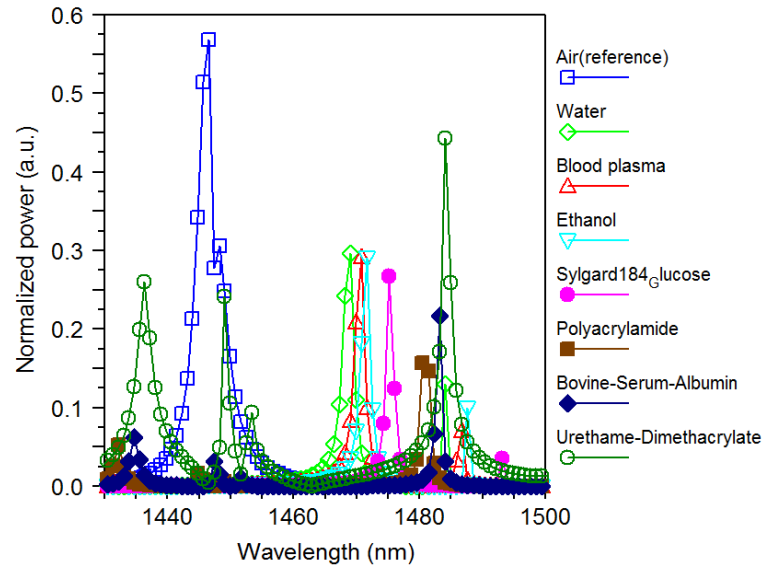


Figure 4.6: The transmission spectra of the biosensor for 18 functional rods.

Table 4.3: Summarizes the results obtained by the biosensor during the conduction of refractive indices of blood components in the case of N=18.

| Name | RI | $\Delta\lambda_{FWHM}$ | λ | Q | S | LD | FOM |
|-------------------------|-------|------------------------|-----------|---------|-------|---------|-------|
| Reference (Air) | 1 | 2.8 | 1446.6 | 516.64 | - | - | - |
| Water | 1.33 | 2.1 | 1469 | 699.52 | 67.87 | 0.0030 | 32.32 |
| Blood Plasma | 1.35 | 2 | 1470.8 | 735.40 | 69.14 | 0.0028 | 34.57 |
| Ethanol | 1.36 | 1.8 | 1471.8 | 817.66 | 67.77 | 0.00250 | 38.88 |
| Sylgard184-Glucose | 1.4 | 1.4 | 1475.1 | 1053.64 | 71.25 | 0.0019 | 50.89 |
| Polyacrylamide | 1.452 | 2 | 1480.5 | 740.25 | 75 | 0.0026 | 37.50 |
| Bovine-Serum-Albumin | 1.47 | 1.2 | 1483.1 | 1235.91 | 77.65 | 0.00154 | 64.71 |
| Urethane-Dimethacrylate | 1.481 | 1.2 | 1484.2 | 1236.83 | 78.17 | 0.00153 | 65.14 |

-1.RI= Refractive index (RIU) -2. $\Delta\lambda_{FWHM}$ =the displacement of the transmission spectrum (RIU)-3.
 λ =Resonance wavelength (nm) -4.Q=Quality factor -5. S=Sensitivity (nm/RIU) -6. DL=Detection limit
 (RIU) -7. FOM=Merit factor (RIU)⁻¹

4.2.4 Case4: Number of rods connected to the biomolecules is 54 rods

In this case, we selected 54 measuring rods as biomolecules to study the performance of the photonic biosensor, as shown in figure 4.7. In figure 4.8 shows the output spectra of the biosensor of measuring rods 54.

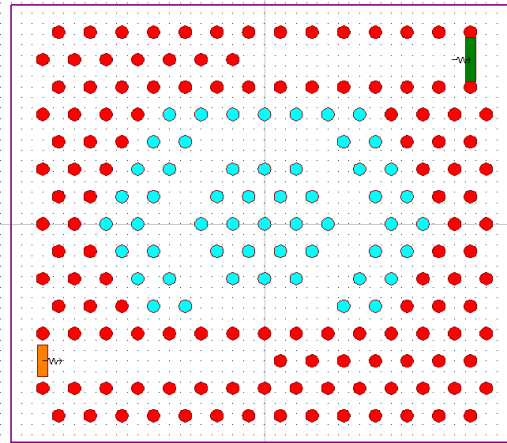


Figure 4.7: The structure of the biosensor for 54 measuring rods.

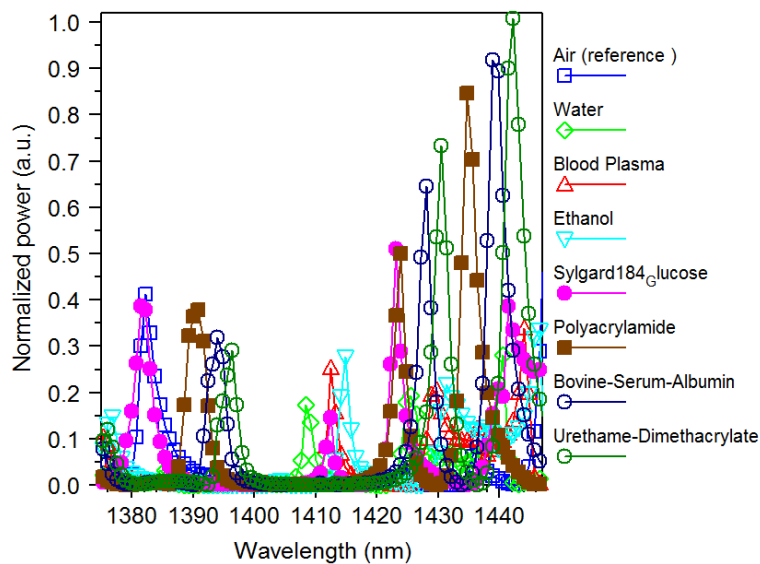


Figure 4.8: The transmission spectra of the biosensor for 54 functional rods.

The table 4.4 presents the simulation results showing that the maximum value of the FOM obtained was $56.527 \text{ (RIU)}^{-1}$, with a sensitivity of 101.75 nm/RIU and a quality factor of 790.555 . This value represents our highest performance, with a refractive index of 1.4 RIU . On the other hand, the minimum value of the FOM was $32.037 \text{ (RIU)}^{-1}$, with a sensitivity of 124.948 nm/RIU and a quality factor of 369.846 . This value represents the lowest performance we have obtained, with a refractive index of 1.481 RIU . The maximum value of DL obtained was 0.0031 RIU , with the same sensitivity and the same previous quality factor for a wavelength of 1442.2 nm .

Table 4.4: Summarizes the results obtained by the biosensor during the conduction of refractive indices of blood components in the case of N=54.

| Name | RI | $\Delta\lambda_{FWHM}$ | λ | Q | S | LD | FOM |
|-------------------------|-------|------------------------|-----------|---------|--------|--------|-------|
| Reference (Air) | 1 | 2.8 | 1382.3 | 439.67 | - | - | - |
| Water | 1.33 | 1.9 | 1408.4 | 741.26 | 79.09 | 0.0024 | 41.62 |
| Blood Plasma | 1.35 | 1.8 | 1412.4 | 7854.66 | 86 | 0.0020 | 47.77 |
| Ethanol | 1.36 | 1.9 | 1414.9 | 744.68 | 90 | 0.0021 | 47.36 |
| Sylgard184-Glucose | 1.4 | 1.8 | 1423 | 790.55 | 101.75 | 0.0017 | 56.52 |
| Polyacrylamide | 1.452 | 2.8 | 1434.7 | 512.39 | 116.18 | 0.0024 | 41.49 |
| Bovine-Serum-Albumin | 1.47 | 3.5 | 1438.8 | 411.08 | 120.21 | 0.0029 | 34.34 |
| Urethane-Dimethacrylate | 1.481 | 3.9 | 1442.2 | 369.84 | 124.94 | 0.0031 | 32.03 |

-1.RI= Refractive index (RIU) -2. $\Delta\lambda_{FWHM}$ =the displacement of the transmission spectrum (nm)-3.
 λ =Resonance wavelength (nm)-4.Q=Quality factor -5. S=Sensitivity (nm/RIU) -6. DL=Detection limit (RIU) -7. FOM=Merit factor (RIU)⁻¹

Figure 4.9 shows the evolution of the quality factor and sensitivity about the number of measuring rods. This figure indicates that the sensitivity increases while the quality factor decreases by changing the number of measuring rods. So, it is necessary to choose a compromise between sensitivity and quality factor. As a result, the optimal quality factor is 1236.83 and the sensitivity is 78.170 for 18 rods.

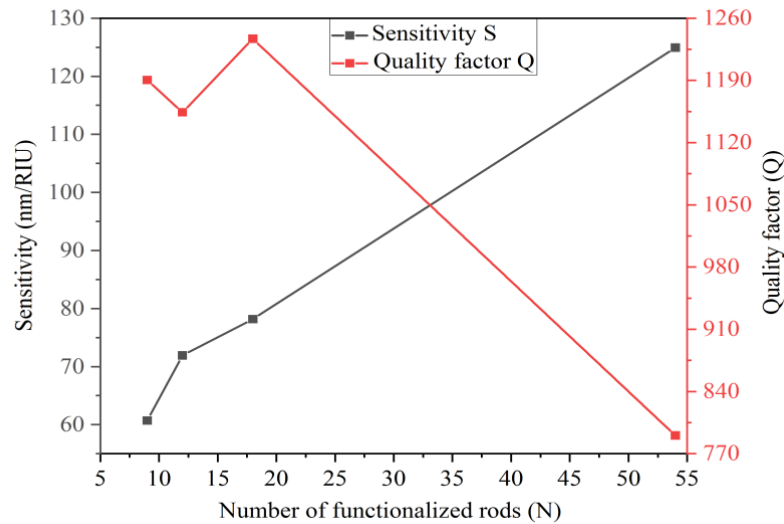


Figure 4.9: The evolution of the quality factor and sensitivity about the number of functional rods (N).

Figure 4.10 assuming that the relationship between sensitivity and the number of measuring rods is approximately linear. The following equation describes the change in the sensitivity value in terms of the number of functional rods after linear adjustment of the simulation data 4.1:

$$S = 1.348 \times N + 52.57 \quad (4.1)$$

The correlation coefficient given by $R^2 = 0.988$ leads us to the conclusion that there is a good correlation between the sensitivity values calculated by the simulator and the linear adjustment of the straight line. The table 4.5 represents the output results of the studied biosensors at a refractive index of 1.484 for the selection of an effective biosensor

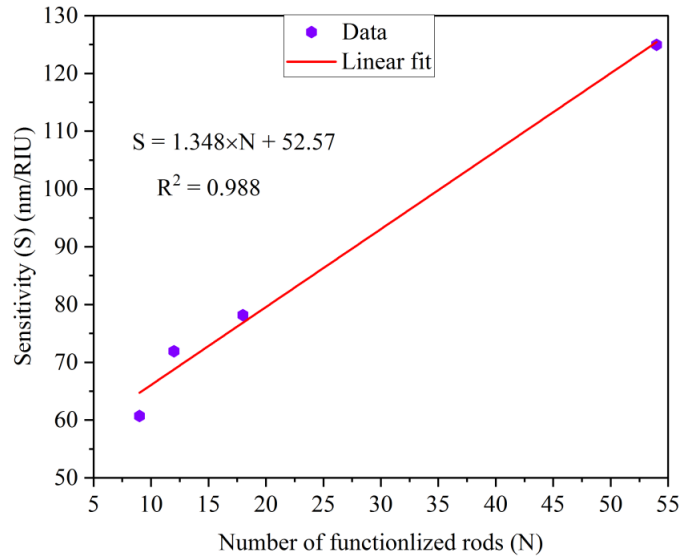


Figure 4.10: Sensitivity to the biosensor as a function of the number of measuring rods (N) for the optimal structure of the biosensor.

Table 4.5: comparison of the results of the main parameters of the studied structures at Urethane-Dimethacrylate.

| N | Q | S | DL | FOM | RI |
|----|---------|--------|---------|-------|-------|
| 9 | 916.23 | 60.70 | 0.0028 | 35.29 | 1.481 |
| 12 | 945.81 | 71.93 | 0.00222 | 44.95 | 1.481 |
| 18 | 1236.83 | 78.17 | 0.00153 | 65.14 | 1.481 |
| 54 | 369.84 | 124.94 | 0.0031 | 32.03 | 1.481 |

-1.N= Measuring rods -2.Q= Quality factor -3. S=Sensitivity (nm/UIR) -4. DL=Detection limit(UIR) -5.RI= Refractive index.

Figure 4.11 (a) presents the curve of the sensitivity mass in terms of the number of measuring rods. 4.11 (b) presents the curve of the relationship between the shift of the resonance wavelength as a function of the number of measuring rods. We observe that the wavelength displacement increases when the number of measuring rods increases while the sensitivity mass decreases. We conclude that the sensitivity mass is inversely proportional to the sensitivity value.

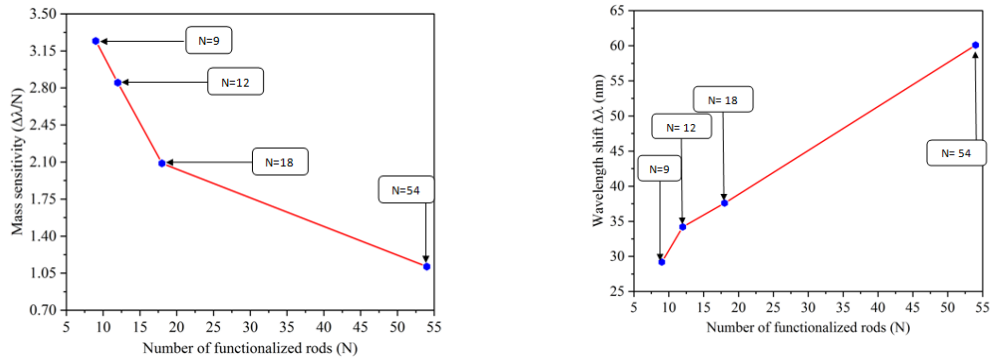


Figure 4.11: (a) Sensitivity mass curve regarding the number of measuring rods. (b) curve the relationship between the wavelength of the variable resonance and the number of measuring rods.

4.3 Comparison of the proposed biosensor with different designs with PCs bases

In table 4.6 our biosensor works better because it has a minimum DL of 0.00153 RIU and an excellent sensitivity of 78.17 nm/RIU compared to existing biosensors, as for the quality factor of 1236.83, it was better compared to the first work.

Table 4.6: Results of previous studies compared to the results obtained.

| References | Structure | Q | S | DL | RI | Sensing parameters/RI range |
|------------|-----------|---------|-------|---------|-------|-----------------------------|
| 2019 [50] | PC-2D | 262 | / | 0.002 | 1.481 | Blood components |
| 2022 [19] | PC-2D | 5166 | 2.94 | 0.021 | 1.481 | Blood components |
| Our work | PC-2D | 1236.83 | 78.17 | 0.00153 | 1.481 | Blood components |

-1.Q= Quality factor -2. S=Sensitivity (nm/UIR) -3. DL=Detection limit(UIR)

4.4 Conclusion

To study all the functional aspects of the biosensors that we propose, we used the same methods as in the previous chapter with a modification of the number of measuring rods. In a hexagonal structure based on 2D photonic crystals, we have deduced that the best biosensor in terms of characteristics is the biosensor with 18 measuring rods. We found that the sensitivity, the quality factor, and the FOM of the optimal device are approximately a maximum quality factor of 1236.83, an FOM of $65.141 \text{ (RIU)}^{-1}$ with sensitivity 78.170 nm/RIU.

General conclusion

Studies carried out in recent years using photonic crystals have shown that they can offer many medical applications as biosensors for optical reading. In optical communication, most research uses the photonic band gap for applications where disease detection and medical diagnosis are made possible thanks to optical detection technology. The basic design of a biosensor consists of trapping light by causing it to propagate through a cavity. This difference in refractive index leads to a shift in the resonance frequency.

Our work aims to optimize the biosensor structure proposed in a two-dimensional hexagonal lattice based on photonic crystals by changing the number of measuring rods to improve sensitivity and quality. In our work, we relied on developing the biosensor structure by coupling the waveguide under the cavity and above in parallel. We used two methods for the simulation. The first method is Band Solve based on the plane wave method (PWE) to optimize the physical dimensions of the studied structure, and the second method is a Full Wave based on the finite differences method in the two-dimensional time domain (FDTD-2D) to control the propagation of light, using the simulation program RSOFT CAD.

As part of this study, to discover how the number of measuring rods affects the improvement of sensitivity and the merit factor, we simulated a biosensor in a 2D hexagonal lattice based on photonic crystals packed 15×15 silicon rods in an air background. The simulation of the proposed biosensor gave a quality factor and a sensitivity of 1190.461 and 60.706 nm/UIR, respectively. To improve the biosensor sensitivity ratio, we increased the number of measuring rods each time; the results showed an increase in the sensitivity value and a variation in the quality factor, reaching a value of about 124.948 nm/UIR and 1236.833, respectively. After the study, we concluded that the 18-rod biosensor with a quality factor of 1236.833, a sensitivity of 78.1704 nm/UIR, and FOM up to $65.141 \text{ (RIU)}^{-1}$ billion was the optimal biosensor.

Finally, we conclude that the measuring rods impact the biosensors characteristics regarding sensitivity and quality factors. From these results, it is possible to identify some exciting points of view since the biosensor structures can be developed in several ways, such as a modification of the number of measuring rods and cavities [17], which makes the biosensors more accurate and efficient.

Bibliography

- [1] E. Yablonovitch, “Photonic band-gap structures,” *JOSA B*, vol. 10, no. 2, pp. 283–295, 1993.
- [2] D. J. John, D. Joannopoulos, J. N. Winn, and R. D. Meade, “Photonic crystals: molding the flow of light,” *In Princeton University of Press: Princeton, NJ, USA*, 2008.
- [3] D. Benelarbi and T. Bouchemat, *Étude de cristaux photoniques en silicium pour l’application à la biodétection*. PhD thesis, Thèse de Doctorat, Université de CONSTANTINE, 2018.
- [4] F. KIHელი and K. DJEBRIT, “Conception des diviseurs de puissance optique 1x2, 1x3 et 1x4 à base des cristaux photoniques,” Master’s thesis, UNIVERSITÉ KASDI MERBAH OUARGLA, 2020.
- [5] D. Leuenberger, “Experimental and numerical investigation of two-dimensional photonic crystals for application in integrated optics,” tech. rep., EPFL, 2004.
- [6] M. E.-F. Hathat, M. Boulesbaa, and S. Gamouh, “Design of new y splitter based on photonic crystal for optical communication,” in *2020 1st International Conference on Communications, Control Systems and Signal Processing (CCSSP)*, pp. 552–556, IEEE, 2020.
- [7] M. Boulesbaa, M. Hathat, A. Bounegab, and O. O. Haddar, “Improvement of optical characteristics of silicon based 1×3 beam splitter with photonic crystal waveguide,” in *AIP Conference Proceedings*, vol. 2440, AIP Publishing, 2022.
- [8] M. E. Hathat, M. Boulesbaa, and S. Gamouh, “Effect of pmma temperature on optical performances of 1×2 hybrid photonic crystals waveguide beam splitters,” *Journal of nano- and electronic physics*, vol. 15, no. 5, p. 05006(5cc), 2023.
- [9] S. Noda, K. Kitamura, T. Okino, D. Yasuda, and Y. Tanaka, “Photonic-crystal surface-emitting lasers: Review and introduction of modulated-photonic crystals,” *IEEE Journal of Selected Topics in Quantum Electronics*, vol. 23, no. 6, pp. 1–7, 2017.
- [10] C. Wiesmann, K. Bergenek, N. Linder, and U. T. Schwarz, “Photonic crystal leds—designing light extraction,” *Laser & Photonics Reviews*, vol. 3, no. 3, pp. 262–286, 2009.
- [11] M. DAOUI, O. ELHELLA, and M. BOULESBAA, “Etude et conception des capteurs ‘à base de cristaux photoniques pour la détection de la pression,” Master’s thesis, UNIVERSITY OF KASDI MERBAH OUARGLA, 2023.

- [12] A. AMOUMENE and I. HALASSA, "Etude et conception des capteurs à base de cristaux photoniques pour la détection de la température," Master's thesis, UNIVERSITY OF KASDI MERBAH OUARGLA, 2022.
- [13] Y.-n. Zhang, Y. Zhao, and R.-q. Lv, "A review for optical sensors based on photonic crystal cavities," *Sensors and Actuators A: Physical*, vol. 233, pp. 374–389, 2015.
- [14] F. Parandin, F. Heidari, Z. Rahimi, and S. Olyaei, "Two-dimensional photonic crystal biosensors: A review," *Optics & laser technology*, vol. 144, p. 107397, 2021.
- [15] D. ELBAHI, *Développement et modélisation de (bio) capteurs électrochimiques pour la détection de l'Amlodipine et de la Pénicilline en phase aqueuse*. PhD thesis, PhD thesis, BADJI MOKHTAR UNIVERSITY, 2019.
- [16] B. Lombardet, "Etude et réalisation de cristaux photoniques pour l'optique intégrée," tech. rep., EPFL, 2005.
- [17] M. BOULESBAA, A. Guermache, and A. Ouali, *Étude et conception de biocapteurs à cristaux photoniques 2D basés sur un guide d'ondes couplé à des cavités*. PhD thesis, UNIVERSITY OF KASDI MERBAH OUARGLA.
- [18] S. K. Roy and P. Sharan, "Photonic crystal based sensor for dna analysis of cancer detection," in *Silicon Photonics & High Performance Computing: Proceedings of CSI 2015*, pp. 79–85, Springer, 2018.
- [19] F. Parandin, F. Heidari, M. Aslinezhad, M. M. Parandin, S. Roshani, and S. Roshani, "Design of 2d photonic crystal biosensor to detect blood components," *Optical and Quantum Electronics*, vol. 54, no. 10, p. 618, 2022.
- [20] S. Sharma, A. Kumar, K. S. Singh, and H. K. Tyagi, "2d photonic crystal based biosensor for the detection of chikungunya virus," *Optik*, vol. 237, p. 166575, 2021.
- [21] S. John, "Strong localization of photons in certain disordered dielectric superlattices," *Physical review letters*, vol. 58, no. 23, p. 2486, 1987.
- [22] E. Yablonovitch, "Inhibited spontaneous emission in solid-state physics and electronics," *Physical review letters*, vol. 58, no. 20, p. 2059, 1987.
- [23] F. Poli, A. Cucinotta, and S. Selleri, *Photonic crystal fibers: properties and applications*, vol. 102. Springer Science & Business Media, 2007.
- [24] J. Carvalho, F. Magalhães, O. Ivanov, O. Frazão, F. Araújo, L. Ferreira, and J. Santos, "Evaluation of coupling losses in hollow-core photonic crystal fibres," in *Third European Workshop on Optical Fibre Sensors*, vol. 6619, pp. 323–326, SPIE, 2007.
- [25] J. Knight, T. Birks, P. S. J. Russell, and D. Atkin, "All-silica single-mode optical fiber with photonic crystal cladding," *Optics letters*, vol. 21, no. 19, pp. 1547–1549, 1996.
- [26] R. D. V. Meade, S. G. Johnson, and J. N. Winn, "Photonic crystals: Molding the flow of light," 2008.
- [27] B. Wild, "Etude expérimentale des propriétés optiques des cristaux photoniques bidimensionnels et de leur accordabilité," tech. rep., EPFL, 2006.

- [28] T. Bouchemat-Boumaza and F. Bougriou, "Etude theorique des materiaux a bandes interdites photoniques bidimensionnels," 2013.
- [29] S. Shaari and A. J. Adnan, "Photonic crystal multiplexer/demultiplexer device for optical communications," in *Frontiers in guided wave optics and optoelectronics*, IntechOpen, 2010.
- [30] Z. Zhang and S. Satpathy, "Electromagnetic wave propagation in periodic structures: Bloch wave solution of maxwell's equations," *Physical review letters*, vol. 65, no. 21, p. 2650, 1990.
- [31] J. Foresi, P. R. Villeneuve, J. Ferrera, E. Thoen, G. Steinmeyer, S. Fan, J. Joannopoulos, L. Kimerling, H. I. Smith, and E. Ippen, "Photonic-bandgap microcavities in optical waveguides," *nature*, vol. 390, no. 6656, pp. 143–145, 1997.
- [32] D. Labilloy, H. Benisty, C. Weisbuch, T. Krauss, V. Bardinal, and U. Oesterle, "Demonstration of cavity mode between two-dimensional photonic-crystal mirrors," *Electronics Letters*, vol. 33, no. 23, pp. 1978–1980, 1997.
- [33] A. Scherer, O. Painter, B. d'Urso, R. Lee, and A. Yariv, "Ingaasp photonic band gap crystal membrane microresonators," *Journal of Vacuum Science & Technology B: Microelectronics and Nanometer Structures Processing, Measurement, and Phenomena*, vol. 16, no. 6, pp. 3906–3910, 1998.
- [34] C. Sauvan, P. Lalanne, and J.-P. Hugonin, "Tuning holes in photonic-crystal nanocavities," *Nature*, vol. 429, no. 6988, pp. 1–1, 2004.
- [35] J. D. Joannopoulos, S. G. Johnson, J. N. Winn, and R. D. Meade, "Molding the flow of light," *Princet. Univ. Press. Princeton, NJ [ua]*, 2008.
- [36] E. Kuramochi, M. Notomi, S. Mitsugi, A. Shinya, T. Tanabe, and T. Watanabe, "Ultrahigh-q photonic crystal nanocavities realized by the local width modulation of a line defect," *Applied physics letters*, vol. 88, no. 4, 2006.
- [37] S. Combri , A. De Rossi, Q. V. Tran, and H. Benisty, "Gaas photonic crystal cavity with ultrahigh q: microwatt nonlinearity at 1.55 μm ," *Optics letters*, vol. 33, no. 16, pp. 1908–1910, 2008.
- [38] S. L. SAOUCHEA, *Cristaux photoniques pour la r alisation de capteur de basse pression. 2018*. PhD thesis, Th ese de doctorat. Universit  Mohamed Boudiaf-M'sila.
- [39] G. Asch and B. Poussery, *Les capteurs en instrumentation industrielle-8e  d.* Dunod, 2017.
- [40] J. Topol'an ik, P. Bhattacharya, J. Sabarinathan, and P.-C. Yu, "Fluid detection with photonic crystal-based multichannel waveguides," *Applied physics letters*, vol. 82, no. 8, pp. 1143–1145, 2003.
- [41] A. Elkous, Z. Bailiche, and H. BENSALAH, "Etude et conception d'un biocapteur   base de cristaux photoniques," 2021.
- [42] F. Karoun, *Etude du comportement de la polyaniline exposee aux gaz polluants*. PhD thesis, Universit  Ferhat Abbas, 2014.

- [43] A. Harhouz, *Contribution à l'étude et la conception des capteurs à base de cristaux photoniques*. PhD thesis, Université Mohamed Boudiaf de M'sila, 2017.
- [44] S. Patel, R. Nanda, S. Sahoo, and E. Mohapatra, "Biosensors in health care: the milestones achieved in their development towards lab-on-chip-analysis," *Biochemistry research international*, vol. 2016, no. 1, p. 3130469, 2016.
- [45] N. A. Mohammed, M. M. Hamed, A. A. Khalaf, and S. El-Rabaie, "Malaria biosensors with ultra-sensitivity and quality factor based on cavity photonic crystal designs," *The European Physical Journal Plus*, vol. 135, no. 11, p. 933, 2020.
- [46] H. Miyan, R. Agrahari, S. K. Gowre, M. Mahto, and P. K. Jain, "Computational study of a compact and high sensitive photonic crystal for cancer cells detection," *IEEE Sensors Journal*, vol. 22, no. 4, pp. 3298–3305, 2022.
- [47] S. Arafa, M. Bouchemat, T. Bouchemat, A. Benmerkhi, and A. Hocini, "Infiltrated photonic crystal cavity as a highly sensitive platform for glucose concentration detection," *Optics Communications*, vol. 384, pp. 93–100, 2017.
- [48] L. Huang, H. Tian, J. Zhou, Q. Liu, P. Zhang, and Y. Ji, "Label-free optical sensor by designing a high-q photonic crystal ring-slot structure," *Optics Communications*, vol. 335, pp. 73–77, 2015.
- [49] N. A. Mohammed, O. E. Khedr, E.-S. M. El-Rabaie, and A. A. Khalaf, "Brain tumors biomedical sensor with high-quality factor and ultra-compact size based on nanocavity 2d photonic crystal," *Alexandria Engineering Journal*, vol. 64, pp. 527–540, 2023.
- [50] R. Arunkumar, T. Suaganya, and S. Robinson, "Design and analysis of 2d photonic crystal based biosensor to detect different blood components," *Photonic Sensors*, vol. 9, pp. 69–77, 2019.